at E9.5, *Mkk4*$^{-/-}$ *Mkk7*$^{+/-}$ embryos were more severely affected than *Mkk4*$^{+/-}$ *Mkk7*$^{-/-}$ embryos. These observations indicate that MKK4 is critical for murine embryogenesis, and that the functions of both MKK4 and MKK7 are required for mammalian body plan organization.

Zebrafish. We originally turned to studying MKK4 and MKK7 in zebrafish because our *Mkk4*$^{-/-}$ *Mkk7*$^{-/-}$ mouse embryos exhibited retarded growth and extremely small body size at E8.5, making it very difficult to analyse the precise nature of MKK4 and MKK7's functions in organizing the vertebrate body plan. Fertilized zebrafish eggs develop *ex utero* into transparent embryos that can be directly observed and are highly amenable to manipulations such as tissue transplantation and molecular perturbation. There is a high degree of conservation between zebrafish and mammalian genes, and a shared developmental path that results in fundamental similarities in many tissues and organs (*54*, *55*). In addition, there exists a wide selection of mutant zebrafish lines with developmental abnormalities, including gastrulation defects. Thus, zebrafish provide a very attractive alternative to mice for studying the molecular and cellular bases of vertebrate morphogenesis.

As introduced above, the zebrafish has two *mkk4* genes, *mkk4a* and *mkk4b*, but only one *mkk7*

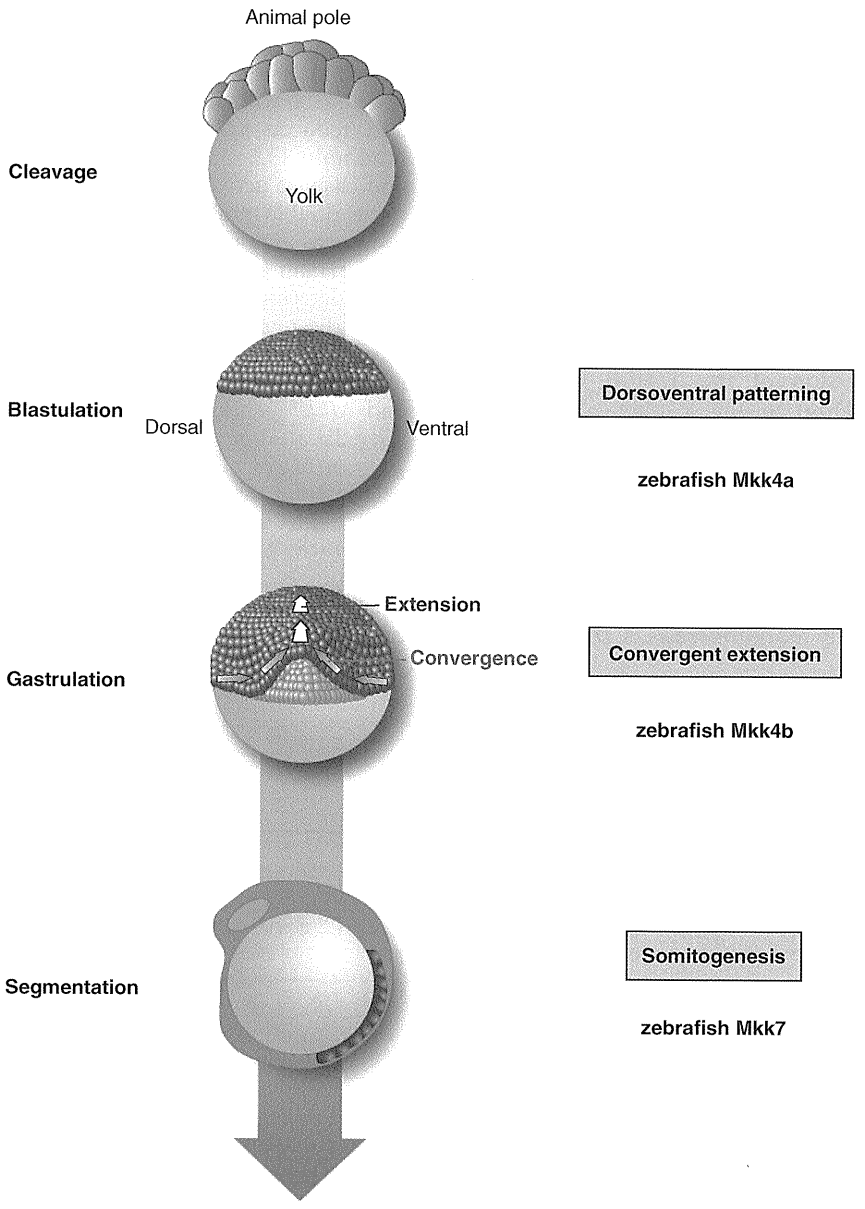

Fig. 5 Multiple roles of zebrafish Mkk4 and Mkk7 during body plan formation. The early embryonic development of the zebrafish occurs in four stages: cleavage, blastulation, gastrulation and segmentation. As indicated, Mkk4a is crucial for dorsoventral patterning, Mkk4b for convergent extension and Mkk7 for somitogenesis.

orthologue. When we used morpholino (MO)-mediated knockdown to examine zebrafish *mkk* gene functions, we found that *mkk4b* MO-injected embryos exhibited axial tissues, which were abnormally short and wide due to defective convergent extension (CE), a driving force of vertebrate gastrulation (Fig. 5). During CE, mesodermal cells migrate towards the future dorsal side of the embryo by means of highly directed and integrated movements, resulting in an overall medio-lateral narrowing (convergence) and anterior– posterior elongation (extension) of the embryo (*54*, *56*, *57*). Previous studies in *Xenopus* and zebrafish have shown that Wnt5 and Wnt11 ligands can signal through a non-canonical Wnt pathway via JNK to influence CE movements during gastrulation (*54*, *56*, *58*, *59*). Surprisingly, *mkk4b* morphants displayed marked up-regulation of *wnt11*, providing the first evidence that *wnt11* itself is a downstream target of the JNK cascade in the non-canonical Wnt pathway associated with early embryogenesis (*60*). More detailed studies revealed that Mkk4b-JNK signalling suppressed *wnt11* expression in a non-cell-autonomous fashion. Our findings suggest that the suppression of *wnt11* transcription by Mkk4b-JNK activation is important for precise regulation of CE.

When we examined our *mkk7* morphants, we found that they had no phenotype during gastrulation but showed abnormal somite morphologies during segmentation (Fig. 5). Mkk7 is thus critical for a slightly later stage of development than is Mkk4b. With respect to Mkk4a, Rui *et al.* (*61*) demonstrated that this kinase participates in dorsoventral patterning in zebrafish blastulas. Mkk4a knockdown reduced the expression of dorsal markers but expanded the expression of ventral markers.

Table I. Physiological roles of MKK4 and MKK7 in development: insights from animal models.

Molecules	Functions	References
Mouse MKK4	Hepatogenesis	(*46*, *48*, *50*)
	Alignment of the Purkinje cells in the cerebellum, radial migration in the cerebral cortex	(*62*)
Mouse MKK7	Hepatogenesis	(*49*)
Chicken MKK4	Not determined	
Xenopus MKK4	Not determined	
Xenopus MKK7	Convergent extension	(*58*)
Zebrafish Mkk4a	Dorsoventral patterning	(*61*)
Zebrafish Mkk4b	Convergent extension	(*60*)
Zebrafish Mkk7	Somitogenesis	(*60*)
Drosophila MKK4	Not detected[a]	(*45*)
Drosophila MKK7	Dorsal closure	(*35–37*)
Caenorhabditis elegans MKK-4	Not detected	(*34*)
Caenorhabditis elegans MEK-1[b]	Not detected	(*33*, *34*)
Caenorhabditis elegans JKK-1[b]	Not detected	(*32*, *34*)

[a]Mutation of this gene results in no detectable abnormal phenotype.
[b]MKK7 paralogue.

Conclusion

JNK activation by MKK4 and MKK7 is a mechanism utilized in parallel morphogenetic events among widely divergent species (Table I). The available data raise the possibility that, in both vertebrates and invertebrates, JNK signalling involving MKK homologues regulates the expression of secreted signalling molecules capable of promoting concerted movements of neighbouring cells (*60*), such as are required in dorsal closure, and cell movements during gastrulation. In *Drosophila*, MKK7 is the principal activator of JNK in the process of dorsal closure. In contrast, our recent researches show that both MKK4 and MKK7 are essential in the multiple processes of body plan formation in mice and zebrafish. The functional properties of MKK4-JNK and MKK7-JNK signalling modules may be governed in part by scaffold proteins that confer specificity to kinase actions. In the future, studies of MAPKKs in other species may reveal more about the evolutionary process by which the partitioning of functions between MKK4 and MKK7 has developed.

Funding
This work was supported by grants from the Japan Society for the Promotion of Science, the Ministry of Education, Culture, Sports, Science and Technology of Japan, and the Ministry of Health, Labor and Welfare of Japan.

Conflict of interest
None declared.

References

1. Manning, A.M. and Davis, R.J. (2003) Targeting JNK for therapeutic benefit: from junk to gold? *Nat. Rev. Drug Discov.* **2**, 554–565
2. Chang, L. and Karin, M. (2001) Mammalian MAP kinase signalling cascades. *Nature* **410**, 37–40
3. Davis, R.J. (2000) Signal transduction by the JNK group of MAP kinases. *Cell.* **103**, 239–252
4. Weston, C.R. and Davis, R.J. (2002) The JNK signal transduction pathway. *Curr. Opin. Genet. Dev.* **12**, 14–21
5. Yashar, B.M., Kelley, C., Yee, K., Errede, B., and Zon, L.I. (1993) Novel members of the mitogen-activated protein kinase activator family in Xenopus laevis. *Mol. Cell Biol.* **13**, 5738–5748
6. Derijard, B., Raingeaud, J., Barrett, T., Wu, I.H., Han, J., Ulevitch, R.J., and Davis, R.J. (1995) Independent human MAP-kinase signal transduction pathways defined by MEK and MKK isoforms. *Science* **267**, 682–685
7. Sanchez, I., Hughes, R.T., Mayer, B.J., Yee, K., Woodgett, J.R., Avruch, J., Kyriakis, J.M., and Zon, L.I. (1994) Role of SAPK/ERK kinase-1 in the stress-activated pathway regulating transcription factor c-Jun. *Nature* **372**, 794–798
8. Lin, A., Minden, A., Martinetto, H., Claret, F.X., Lange-Carter, C., Mercurio, F., Johnson, G.L., and Karin, M. (1995) Identification of a dual specificity kinase that activates the Jun kinases and p38-Mpk2. *Science* **268**, 286–290
9. Tournier, C., Whitmarsh, A.J., Cavanagh, J., Barrett, T., and Davis, R.J. (1997) Mitogen-activated protein kinase

kinase 7 is an activator of the c-Jun NH2-terminal kinase. *Proc. Natl Acad. Sci. USA* **94**, 7337–7342
10. Yao, Z., Diener, K., Wang, X.S., Zukowski, M., Matsumoto, G., Zhou, G., Mo, R., Sasaki, T., Nishina, H., Hui, C C., Tan, T.H., Woodgett, J.P., and Penninger, J.M. (1997) Activation of stress-activated protein kinases/c-Jun N-terminal protein kinases (SAPKs/JNKs) by a novel mitogen-activated protein kinase kinase. *J. Biol. Chem.* **272**, 32378–32383
11. Moriguchi, T., Toyoshima, F., Masuyama, N., Hanafusa, H., Gotoh, Y., and Nishida, E. (1997) A novel SAPK/JNK kinase, MKK7, stimulated by TNFalpha and cellular stresses. *EMBO J.* **16**, 7045–7053
12. Tournier, C., Whitmarsh, A.J., Cavanagh, J., Barrett, T., and Davis, R.J. (1999) The MKK7 gene encodes a group of c-Jun NH2-terminal kinase kinases. *Mol. Cell Biol.* **19**, 1569–1581
13. Fleming, Y., Armstrong, C.G., Morrice, N., Paterson, A., Goedert, M., and Cohen, P. (2000) Synergistic activation of stress-activated protein kinase 1/c-Jun N-terminal kinase (SAPK1/JNK) isoforms by mitogen-activated protein kinase kinase 4 (MKK4) and MKK7. *Biochem. J.* **352 (Pt 1)**, 145–154
14. Lawler, S., Fleming, Y., Goedert, M., and Cohen, P. (1998) Synergistic activation of SAPK1/JNK1 by two MAP kinase kinases in vitro. *Curr. Biol.* **8**, 1387–1390
15. Lisnock, J., Griffin, P., Calaycay, J., Frantz, B., Parsons, J., O'Keefe, S.J., and LoGrasso, P. (2000) Activation of JNK3 alpha 1 requires both MKK4 and MKK7: kinetic characterization of in vitro phosphorylated JNK3 alpha 1. *Biochemistry* **39**, 3141–3148
16. Wada, T., Nakagawa, K., Watanabe, T., Nishitai, G., Seo, J., Kishimoto, H., Kitagawa, D., Sasaki, T., Penninger, J.M., Nishina, H., and Katada, T. (2001) Impaired synergistic activation of stress-activated protein kinase SAPK/JNK in mouse embryonic stem cells lacking SEK1/MKK4: different contribution of SEK2/MKK7 isoforms to the synergistic activation. *J. Biol. Chem.* **276**, 30892–30897
17. Kishimoto, H., Nakagawa, K., Watanabe, T., Kitagawa, D., Momose, H., Seo, J., Nishitai, G., Shimizu, N., Ohata, S., Tanemura, S., Asaka, S., Goto, T., Fukushi, H., Yoshida, H., Suzuki, A., Sasaki, T., Wada, T., Penninger, J.M., Nishina, H., and Katada, T. (2003) Different properties of SEK1 and MKK7 in dual phosphorylation of stress-induced activated protein kinase SAPK/JNK in embryonic stem cells. *J. Biol. Chem.* **278**, 16595–16601
18. Nishina, H., Wada, T., and Katada, T. (2004) Physiological roles of SAPK/JNK signaling pathway. *J. Biochem.* **136**, 123–126
19. Ho, D.T., Bardwell, A.J., Grewal, S., Iverson, C., and Bardwell, L. (2006) Interacting JNK-docking sites in MKK7 promote binding and activation of JNK mitogen-activated protein kinases. *J. Biol. Chem.* **281**, 13169–13179
20. Ho, D.T., Bardwell, A.J., Abdollahi, M., and Bardwell, L. (2003) A docking site in MKK4 mediates high affinity binding to JNK MAPKs and competes with similar docking sites in JNK substrates. *J. Biol. Chem.* **278**, 32662–32672
21. Dhanasekaran, D.N., Kashef, K., Lee, C.M., Xu, H., and Reddy, E.P. (2007) Scaffold proteins of MAP-kinase modules. *Oncogene* **26**, 3185–3202
22. Dickens, M., Rogers, J.S., Cavanagh, J., Raitano, A., Xia, Z., Halpern, J.R., Greenberg, M.E., Sawyers, C.L., and Davis, R.J. (1997) A cytoplasmic inhibitor of the JNK signal transduction pathway. *Science* **277**, 693–696
23. Yasuda, J., Whitmarsh, A.J., Cavanagh, J., Sharma, M., and Davis, R.J. (1999) The JIP group of mitogen-activated protein kinase scaffold proteins. *Mol. Cell Biol.* **19**, 7245–7254
24. Kelkar, N., Gupta, S., Dickens, M., and Davis, R.J. (2000) Interaction of a mitogen-activated protein kinase signaling module with the neuronal protein JIP3. *Mol. Cell Biol.* **20**, 1030–1043
25. Ito, M., Yoshioka, K., Akechi, M., Yamashita, S., Takamatsu, N., Sugiyama, K., Hibi, M., Nakabeppu, Y., Shiba, T., and Yamamoto, K.I. (1999) JSAP1, a novel jun N-terminal protein kinase (JNK)-binding protein that functions as a Scaffold factor in the JNK signaling pathway. *Mol. Cell Biol.* **19**, 7539–7548
26. Kelkar, N., Standen, C.L., and Davis, R.J. (2005) Role of the JIP4 scaffold protein in the regulation of mitogen-activated protein kinase signaling pathways. *Mol. Cell Biol.* **25**, 2733–2743
27. Lee, C.M., Onesime, D., Reddy, C.D., Dhanasekaran, N., and Reddy, E.P. (2002) JLP: A scaffolding protein that tethers JNK/p38MAPK signaling modules and transcription factors. *Proc. Natl Acad. Sci. USA* **99**, 14189–14194
28. Jagadish, N., Rana, R., Selvi, R., Mishra, D., Garg, M., Yadav, S., Herr, J.C., Okumura, K., Hasegawa, A., Koyama, K., and Suri, A. (2005) Characterization of a novel human sperm-associated antigen 9 (SPAG9) having structural homology with c-Jun N-terminal kinase-interacting protein. *Biochem. J.* **389**, 73–82
29. Xu, Z., Kukekov, N.V., and Greene, L.A. (2003) POSH acts as a scaffold for a multiprotein complex that mediates JNK activation in apoptosis. *EMBO J.* **22**, 252–261
30. Marti, A., Luo, Z., Cunningham, C., Ohta, Y., Hartwig, J., Stossel, T.P., Kyriakis, J.M., and Avruch, J. (1997) Actin-binding protein-280 binds the stress-activated protein kinase (SAPK) activator SEK-1 and is required for tumor necrosis factor-alpha activation of SAPK in melanoma cells. *J. Biol. Chem.* **272**, 2620–2628
31. Nakagawa, K., Sugahara, M., Yamasaki, T., Kajiho, H., Takahashi, S., Hirayama, J., Minami, Y., Ohta, Y., Watanabe, T., Hata, Y., Katada, T., and Nishina, H. (2010) Filamin associates with stress signalling kinases MKK7 and MKK4 and regulates JNK activation. *Biochem. J.* **427**, 237–245
32. Kawasaki, M., Hisamoto, N., Iino, Y., Yamamoto, M., Ninomiya-Tsuji, J., and Matsumoto, K. (1999) A Caenorhabditis elegans JNK signal transduction pathway regulates coordinated movement via type-D GABAergic motor neurons. *EMBO J.* **18**, 3604–3615
33. Koga, M., Zwaal, R., Guan, K.L., Avery, L., and Ohshima, Y. (2000) A Caenorhabditis elegans MAP kinase kinase, MEK-1, is involved in stress responses. *EMBO J.* **19**, 5148–5156
34. Villanueva, A., Lozano, J., Morales, A., Lin, X., Deng, X., Hengartner, M.O., and Kolesnick, R.N. (2001) jkk-1 and mek-1 regulate body movement coordination and response to heavy metals through jnk-1 in Caenorhabditis elegans. *EMBO J.* **20**, 5114–5128
35. Glise, B., Bourbon, H., and Noselli, S. (1995) hemipterous encodes a novel Drosophila MAP kinase kinase, required for epithelial cell sheet movement. *Cell* **83**, 451–461
36. Riesgo-Escovar, J.R., Jenni, M., Fritz, A., and Hafen, E. (1996) The drosophila Jun-N-terminal kinase is required for cell morphogenesis but not for DJun-dependent cell fate specification in the eye. *Genes Dev.* **10**, 2759–2768
37. Sluss, H.K., Han, Z., Barrett, T., Goberdhan, D.C., Wilson, C., Davis, R.J., and Ip, Y.T. (1996) A JNK signal transduction pathway that mediates

morphogenesis and an immune response in Drosophila. *Genes Dev.* **10**, 2745–2758
38. Hou, X.S., Goldstein, E.S., and Perrimon, N. (1997) Drosophila Jun relays the Jun amino-terminal kinase signal transduction pathway to the Decapentaplegic signal transduction pathway in regulating epithelial cell sheet movement. *Genes Dev.* **11**, 1728–1737
39. Kockel, L., Zeitlinger, J., Staszewski, L.M., Mlodzik, M., and Bohmann, D. (1997) Jun in drosophila development: redundant and nonredundant functions and regulation by two MAPK signal transduction pathways. *Genes Dev.* **11**, 1748–1758
40. Riesgo-Escovar, J.R. and Hafen, E. (1997) Drosophila Jun kinase regulates expression of decapentaplegic via the ETS-domain protein Aop and the AP-1 transcription factor DJun during dorsal closure. *Genes Dev.* **11**, 1717–1727
41. Riesgo-Escovar, J.R. and Hafen, E. (1997) Common and distinct roles of DFos and DJun during Drosophila development. *Science* **278**, 669–672
42. Zeitlinger, J., Kockel, L., Peverali, F.A., Jackson, D.B., Mlodzik, M., and Bohmann, D. (1997) Defective dorsal closure and loss of epidermal decapentaplegic expression in Drosophila fos mutants. *EMBO J.* **16**, 7393–7401
43. Reed, B.H., Wilk, R., and Lipshitz, H.D. (2001) Downregulation of Jun kinase signaling in the amnioserosa is essential for dorsal closure of the Drosophila embryo. *Curr. Biol.* **11**, 1098–1108
44. Han, Z.S., Enslen, H., Hu, X., Meng, X., Wu, I.H., Barrett, T., Davis, R.J., and Ip, Y.T. (1998) A conserved p38 mitogen-activated protein kinase pathway regulates Drosophila immunity gene expression. *Mol. Cell Biol.* **18**, 3527–3539
45. Geuking, P., Narasimamurthy, R., Lemaitre, B., Basler, K., and Leulier, F. (2009) A non-redundant role for Drosophila Mkk4 and hemipterous/Mkk7 in TAK1-mediated activation of JNK. *PLoS One* **4**, e7709
46. Ganiatsas, S., Kwee, L., Fujiwara, Y., Perkins, A., Ikeda, T., Labow, M.A., and Zon, L.I. (1998) SEK1 deficiency reveals mitogen-activated protein kinase cascade crossregulation and leads to abnormal hepatogenesis. *Proc. Natl Acad. Sci. USA* **95**, 6881–6886
47. Nishina, H., Fischer, K.D., Radvanyi, L., Shahinian, A., Hakem, R., Rubie, E.A., Bernstein, A., Mak, T.W., Woodgett, J.R., and Penninger, J.M. (1997) Stress-signalling kinase Sek1 protects thymocytes from apoptosis mediated by CD95 and CD3. *Nature* **385**, 350–353
48. Nishina, H., Vaz, C., Billia, P., Nghiem, M., Sasaki, T., De la Pompa, J.L., Furlonger, K., Paige, C., Hui, C., Fischer, K.D., Kishimoto, H., Iwatsubo, T., Katada, T., Woodgett, J.R., and Penninger, J.M. (1999) Defective liver formation and liver cell apoptosis in mice lacking the stress signaling kinase SEK1/MKK4. *Development* **126**, 505–516
49. Wada, T., Joza, N., Cheng, H.Y., Sasaki, T., Kozieradzki, I., Bachmaier, K., Katada, T., Schreiber, M., Wagner, E.F., Nishina, H., and Penninger, J.M. (2004) MKK7 couples stress signalling to G2/M cell-cycle progression and cellular senescence. *Nat. Cell Biol.* **6**, 215–226
50. Watanabe, T., Nakagawa, K., Ohata, S., Kitagawa, D., Nishitai, G., Seo, J., Tanemura, S., Shimizu, N., Kishimoto, H., Wada, T., Aoki, J., Arai, H., Iwatsubo, T., Mochita, M., Satake, M., Ito, Y., Matsuyama, T., Mak, T.W., Penninger, J.M., Nishina, H., and Katada, T. (2002) SEK1/MKK4-mediated SAPK/JNK signaling participates in embryonic hepatoblast proliferation via a pathway different from NF-kappaB-induced anti-apoptosis. *Dev. Biol.* **250**, 332–347
51. Yang, D., Tournier, C., Wysk, M., Lu, H.T., Xu, J., Davis, R.J., and Flavell, R.A. (1997) Targeted disruption of the MKK4 gene causes embryonic death, inhibition of c-Jun NH2-terminal kinase activation, and defects in AP-1 transcriptional activity. *Proc. Natl Acad. Sci. USA* **94**, 3004–3009
52. Kuan, C.Y., Yang, D.D., Samanta Roy, D.R., Davis, R.J., Rakic, P., and Flavell, R.A. (1999) The Jnk1 and Jnk2 protein kinases are required for regional specific apoptosis during early brain development. *Neuron* **22**, 667–676
53. Sabapathy, K., Jochum, W., Hochedlinger, K., Chang, L., Karin, M., and Wagner, E. F. (1999) Defective neural tube morphogenesis and altered apoptosis in the absence of both JNK1 and JNK2. *Mech. Dev.* **89**, 115–124
54. Tada, M., Concha, M.L., and Heisenberg, C.P. (2002) Non-canonical Wnt signalling and regulation of gastrulation movements. *Semin. Cell Dev. Biol.* **13**, 251–260
55. Keller, R., Davidson, L., Edlund, A., Elul, T., Ezin, M., Shook, D., and Skoglund, P. (2000) Mechanisms of convergence and extension by cell intercalation. *Phil. Trans. R. Soc. Lond. B Biol. Sci.* **355**, 897–922
56. Keller, R. (2002) Shaping the vertebrate body plan by polarized embryonic cell movements. *Science* **298**, 1950–1954
57. Solnica-Krezel, L. (2006) Gastrulation in zebrafish – all just about adhesion? *Curr. Opin. Genet. Dev.* **16**, 433–441
58. Yamanaka, H., Moriguchi, T., Masuyama, N., Kusakabe, M., Hanafusa, H., Takada, R., Takada, S., and Nishida, E. (2002) JNK functions in the non-canonical Wnt pathway to regulate convergent extension movements in vertebrates. *EMBO Rep.* **3**, 69–75
59. Seifert, J.R. and Mlodzik, M. (2007) Frizzled/PCP signalling: a conserved mechanism regulating cell polarity and directed motility. *Nat. Rev. Genet.* **8**, 126–138
60. Seo, J., Asaoka, Y., Nagai, Y., Hirayama, J., Yamasaki, T., Namae, M., Ohata, S., Shimizu, N., Negishi, T., Kitagawa, D., Kondoh, H., Furutani-Seiki, M., Penninger, J.M., Katada, T., and Nishina, H. (2010) Negative regulation of wnt11 expression by Jnk signaling during zebrafish gastrulation. *J. Cell Biochem.* **110**, 1022–1037
61. Rui, Y., Xu, Z., Xiong, B., Cao, Y., Lin, S., Zhang, M., Chan, S.C., Luo, W., Han, Y., Lu, Z., Ye, Z., Zhou, H.M., Han, J., Meng, A., and Lin, S.C. (2007) A beta-catenin-independent dorsalization pathway activated by Axin/JNK signaling and antagonized by aida. *Dev. Cell* **13**, 268–282
62. Wang, X., Nadarajah, B., Robinson, A.C., McColl, B.W., Jin, J.W., Dajas-Bailador, F., Boot-Handford, R.P., and Tournier, C. (2007) Targeted deletion of the mitogen-activated protein kinase kinase 4 gene in the nervous system causes severe brain developmental defects and premature death. *Mol. Cell Biol.* **27**, 7935–7946

Biochemical and Biophysical Research Communications 396 (2010) 887–893

Contents lists available at ScienceDirect

Biochemical and Biophysical Research Communications

journal homepage: www.elsevier.com/locate/ybbrc

The LIM protein Ajuba is required for ciliogenesis and left–right axis determination in medaka

Yoko Nagai [a,b,1], Yoichi Asaoka [a,1], Misako Namae [a], Kota Saito [b], Haruka Momose [b], Hiroshi Mitani [c], Makoto Furutani-Seiki [d], Toshiaki Katada [b], Hiroshi Nishina [a,*]

[a] Department of Developmental and Regenerative Biology, Medical Research Institute, Tokyo Medical and Dental University, Tokyo 113-8510, Japan
[b] Department of Physiological Chemistry, Graduate School of Pharmaceutical Sciences, University of Tokyo, Tokyo 113-0033, Japan
[c] Department of Integrated Biosciences, Graduate School of Frontier Science, University of Tokyo, Chiba 277-8561, Japan
[d] Centre for Regenerative Medicine, Department of Biology and Biochemistry, University of Bath, Claverton Down, Bath BA2 7AY, UK

ARTICLE INFO

Article history:
Received 1 May 2010
Available online 10 May 2010

Keywords:
Ajuba
Cilia
Basal body
Left–right asymmetry
Medaka

ABSTRACT

Cilia are microtubule-based organelles that are present on the surfaces of almost all vertebrate cells. Most cilia function as sensory or molecular transport structures. Malfunctions of cilia have been implicated in several diseases of human development. The assembly of cilia is initiated by the centriole (or basal body), and several centrosomal proteins are involved in this process. The mammalian LIM protein Ajuba is a well-studied centrosomal protein that regulates cell division but its role in ciliogenesis is unknown. In this study, we isolated the medaka homolog of Ajuba and showed that Ajuba localizes to basal bodies of cilia in growth-arrested cells. Knockdown of Ajuba resulted in randomized left–right organ asymmetries and altered expression of early genes responsible for left–right body axis determination. At the cellular level, we found that Ajuba function was essential for ciliogenesis in the cells lining Kupffer's vesicle; it is these cells that induce the asymmetric fluid flow required for left–right axis determination. Taken together, our findings identify a novel role for Ajuba in the regulation of vertebrate ciliogenesis and left–right axis determination.

1. Introduction

Cilia are microtubule-based hair-like organelles that extend from the surfaces of almost all vertebrate cells. Studies over the past decade have revealed that cilia, which can be motile or immotile, play pivotal roles in a wide variety of cellular functions [1]. For example, immotile cilia typically function as specialized sensory structures, such as the olfactory cilia and retinal photoreceptor outer segments. In contrast, the motile cilia located on epithelial cells, including respiratory epithelial cells and brain ependymal cells, transport extracellular fluid along the epithelial surface. In addition, motile cilia at the embryonic node generate an extraembryonic fluid flow that is required to establish embryonic left–right asymmetry [2]. Defects in genes involved in cilia assembly or function have been associated with many diseases of human development, including Bardet Biedl syndrome, hydrocephalus, and *situs inversus* (reversal of normal visceral asymmetry) [3]. These disorders reflect the crucial role of cilia in regulating vertebrate developmental processes.

The assembly of a cilium requires a basal body that is derived from one of the two centrioles that constitute the centrosome [4,5]. During ciliogenesis, the centriole migrates to the plasma membrane and ciliary microtubules elongate from its distal end. Once a centriole has docked with the plasma membrane, it is known as a basal body. Recently, it was reported that certain centrosomal proteins are required for cilium formation [6,7]. We therefore, hypothesized that additional centrosomal proteins might also be involved in regulating vertebrate ciliogenesis.

Ajuba is a conserved centrosomal protein that was originally identified in mice and contains three LIM domains in its C-terminal region [8]. Ajuba contributes to the formation and maintenance of cell–cell junctions [9,10] and plays a role in cell migration [11,12]. Ajuba is also important for mammalian cell division. In humans, the association of Ajuba with the LATS2 protein and microtubules at the centrosome regulates mitotic spindle organization [13–15]. To investigate whether Ajuba is required for the assembly of cilia and vertebrate embryonic development, we exploited a gene knockdown system in the ricefish medaka (*Oryzias latipes*). Medaka embryos develop outside the mother's body, making it easy to inspect them visually and to manipulate their tissues and cells [16]. Here, we provide evidence that Ajuba is required for the assembly of Kupffer's vesicle (KV) cilia and thus for left–right axis determination in developing medaka embryos.

* Corresponding author. Address: 1-5-45 Yushima, Bunkyo-ku, Tokyo 113-8510, Japan. Fax: +81 3 5803 5829.
E-mail address: nishina.dbio@mri.tmd.ac.jp (H. Nishina).
[1] These authors contributed equally to this work.

0006-291X/$ - see front matter © 2010 Elsevier Inc. All rights reserved.
doi:10.1016/j.bbrc.2010.05.017

2. Materials and methods

2.1. Fish maintenance

Embryos and adults of the medaka Cab inbred strain were used for all experiments. Embryos were raised at 30 °C and embryonic stages were determined based on morphological features, as previously described [16].

2.2. Cloning and RT-PCR

Partial or full-length cDNAs of the *ajuba* (GenBank Accession No. AB523732) and *pitx2* (Ensembl ID ENSORLG00000020587) genes were generated by RT-PCR of mRNAs purified from medaka embryos at various stages of development. The primers used in the RT-PCR reactions are shown in Supplemental Table 1 (see Supplemental information online).

2.3. Whole mount in situ hybridization

Whole mount *in situ* hybridization was performed as previously described [17], using antisense digoxigenin (DIG)-labeled riboprobes generated from medaka *ajuba, pitx2, shh,* or *spaw* partial cDNAs. Probes for *spaw* and *shh* were used as previously described [18,19].

2.4. Cell culture and immunofluorescence

cDNA encoding medaka Ajuba was cloned into the expression vector pEGFP-C1; this recombinant EGFP vector was termed GFP-Ajuba. Medaka hepatoma (DIT) cells were grown to 50% confluency on 15-mm diameter glass coverslips in Leibovitz L-15 medium (Sigma) supplemented with 10% FBS (GIBCO) [20]. DIT cells were transfected with 1 μg of GFP-Ajuba plus Fugene HD (Roche) according to the manufacturer's instructions. Transfected cells were grown for 24 h and fixed with 4% paraformaldehyde (PFA) in phosphate-buffered saline (PBS) for 10 min at room temperature (RT). Cells were treated with methanol at −20 °C for at least another 3 min, followed by permeabilizing with 0.2% Triton X-100 in PBS. Permeabilized cells were incubated with blocking solution [5% bovine serum albumin (BSA) in TBS] for 30 min at RT, then for 2 h at 37 °C with blocking solution containing mouse anti-acetylated tubulin monoclonal antibody (1:1000; Sigma) and mouse anti-γ tubulin monoclonal antibody (1:1000; Sigma). Antibody-bound cells were washed with PBS and incubated with Alexa 488-conjugated secondary antibodies for 30 min. After several PBS washes, coverslips were mounted and viewed on a Carl Zeiss confocal microscope equipped with LSM510 software.

2.5. Gene knockdown by morpholinos

Morpholino antisense oligos (MOs) were synthesized by GeneTools, LLC (Philomath, OR). MOs were injected into the cytoplasm of one-cell stage medaka embryos. Sequences of MOs used were as follows:

- Ajuba spMO (splice-blocking), 5′-GCCTT GACCT CAGCT CTTAC CATGT-3′;
- Ajuba augMO (translation-blocking), 5′-GCTTT GTTAT TGGCT TTTCC ATGGT-3′;
- Standard control MO, 5′-CCTCT TACCT CAGTT ACAAT TTATA-3′.

2.6. Immunohistochemistry

Medaka embryos were fixed in 4% PFA/PBST (PBS at pH 7.5 containing 0.1% Tween 20) at 4 °C overnight. The chorion of the embryos was removed and the embryos were washed several times with PBST and stored in methanol at −20 °C until use. Embryos to be used were gradually rehydrated, washed several times with PBST, and blocked in 2% BSA plus 1% DMSO in PBST at RT for 2 h. Blocked embryos were incubated in blocking solution containing anti-mouse acetylated tubulin antibody (1:1000, Sigma T-6793) at 4 °C overnight. After several washes with PBST, embryos were blocked again at RT for 2 h and then incubated with Alexa Fluor 488-conjugated goat anti-mouse IgG antibody (1:1000) at 4 °C overnight. After removal of the tail region, immunostained embryos were mounted in Fluor Save Reagent (Calbiochem) and imaged using a Zeiss LSM scanning laser confocal microscope with a 40× objective.

2.7. Cryosectioning and hematoxylin/eosin staining

Hatched medaka larvae were fixed in 4% PFA/PBS overnight. Fixed embryos were washed in PBS and incubated in 20% sucrose solution in PBS for several days. The infused embryos were then embedded in optimal cutting temperature compound (Tissue-Tek) and cryosectioned at 6 μm. Sections were stained with hematoxylin/eosin and viewed using a Leica DMRA fluorescence microscope.

3. Results

3.1. Expression pattern and localization of medaka Ajuba

We isolated the full-length cDNA of medaka *ajuba* by performing BLAST searches and subsequent RT-PCR. A phylogenetic analysis revealed that the medaka Ajuba shows greater sequence similarity to the mammalian and teleost Ajuba proteins than to other Ajuba-related LIM protein members, Wtip and Limd1 (Fig. 1A) [21]. The predicted amino acid (aa) sequence of medaka Ajuba is 41–43% identical to the aa sequences of the human and mouse Ajuba proteins, and the Ajuba nuclear export signal (NES) and LIM domains are well-conserved among species (Fig. S1). We then examined the expression pattern of *ajuba* during early medaka development using RT-PCR analysis and whole mount *in situ* hybridization. Medaka *ajuba* mRNA was detectable in embryos from stages 17 to 30 (Fig. 1B). At early somite stages (stages 19 and 21), *ajuba* transcripts were broadly expressed, with higher levels observed in the tailbud (Fig. 1C, Fig. S2). At later somite stages (stages 25 and 30), expression of *ajuba* mRNA became more localized in the developing retina and several brain areas. These observations suggest that medaka *ajuba* is expressed in multiple ciliated tissues during early development.

To determine the localization of Ajuba protein in cells, we transfected EGFP-tagged medaka Ajuba (GFP-Ajuba) into medaka DIT cells and performed immunofluorescence analysis. Because primary cilia grow only at interphase, cells were cultured under low serum (0.5%) conditions to limit proliferative growth. In growth-arrested DIT cells, GFP-Ajuba co-localized with the centrosome/basal body marker γ-tubulin, although additional GFP-Ajuba granules could be seen scattered in the cytoplasm (Fig. 1D). This co-localization of medaka Ajuba with γ-tubulin is consistent with results reported for mammalian cells [13,14].

3.2. Knockdown of medaka ajuba disrupts the laterality of internal organs

To identify the physiological function of Ajuba during medaka embryogenesis, we designed translation- and splice-blocking morpholinos (augMO and spMO, respectively) to knock down *ajuba* mRNA and block Ajuba protein expression (Fig. 2A). To confirm

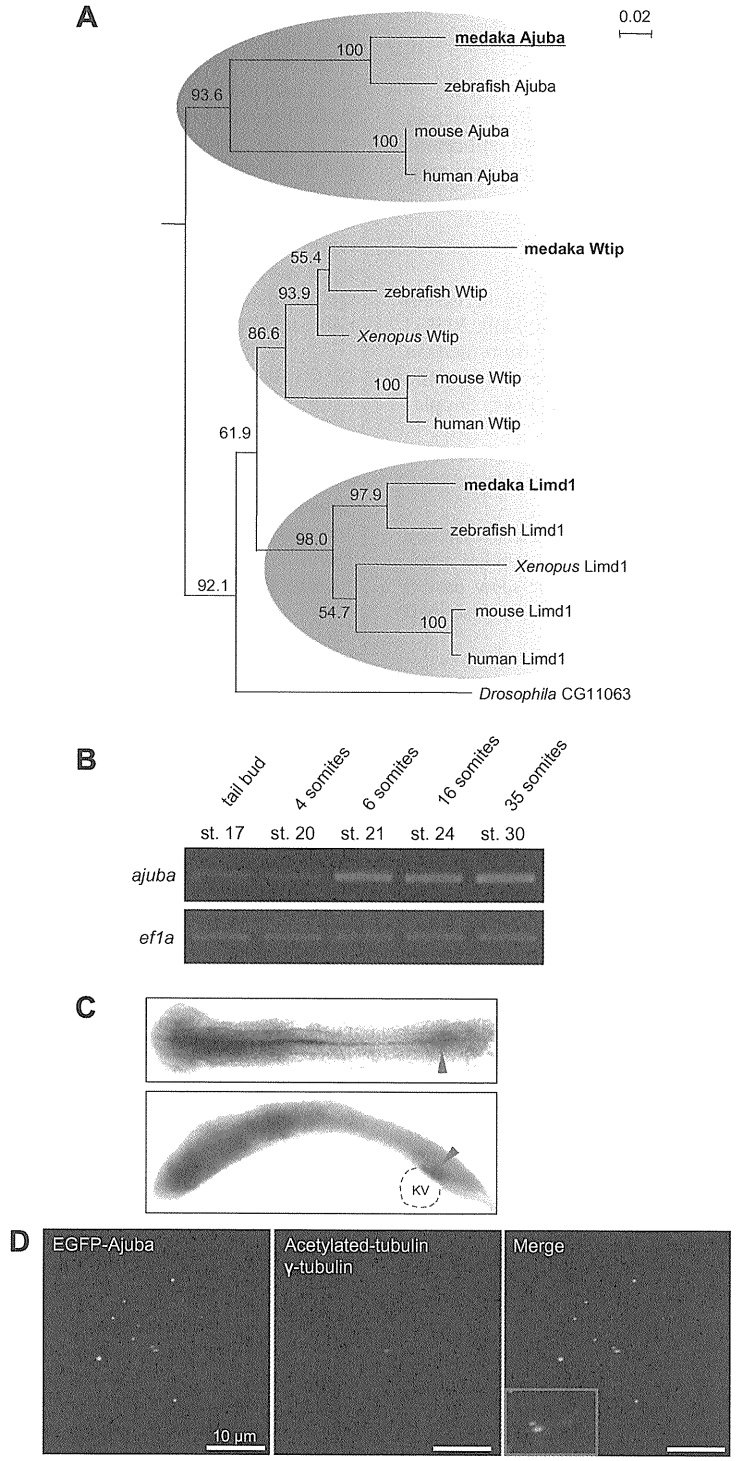

Fig. 1. Cloning of the medaka *ajuba* gene and localization of the Ajuba mRNA and protein in medaka embryos and cultured cells. (A) Phylogenetic classification of medaka Ajuba/Wtip/Limd1 proteins. Three medaka Ajuba/Wtip/Limd1 proteins were classified as members of the indicated vertebrate LIM families on the basis of amino acid (aa) sequence. The deepest roots of the trees were determined using the sequence of the *Drosophila* Zyxin homolog as an outgroup. The estimated bootstrap probabilities (percent) of local topologies are shown on each node. The length of the scale bar corresponds to an evolutionary distance of 0.02 aa substitution per site (2% sequence difference). (B) Broad expression of *ajuba* mRNA during early medaka development. RT-PCR analysis of *ajuba* expression was performed in WT medaka embryos at the indicated stages. *ef1a*, loading control. (C) Prominent Ajuba expression in the tailbud. A stage 21 medaka embryo was examined by whole mount *in situ* hybridization to detect *ajuba* mRNA. Upper panel, dorsal view; bottom panel, lateral view. Anterior of both embryos is to the left. Ajuba was broadly expressed but the higher levels were seen in cells (arrowheads) in the areas adjacent to the KV (outlined with dotted line). (D) Localization of Ajuba in the basal body of cilia. Medaka DIT cells were transfected with GFP-Ajuba and immunostained with anti-acetylated tubulin and anti-γ tubulin (red), which are the ciliary marker and the basal body marker, respectively. Localization of Ajuba protein was determined by immunofluorescence microscopy. A GFP-Ajuba granule was located at the basal body of cilia, but most were scattered in the cytoplasm. Inset, magnified image of co-stained basal body and cilium. For all Figures, results shown are representative of six trials.

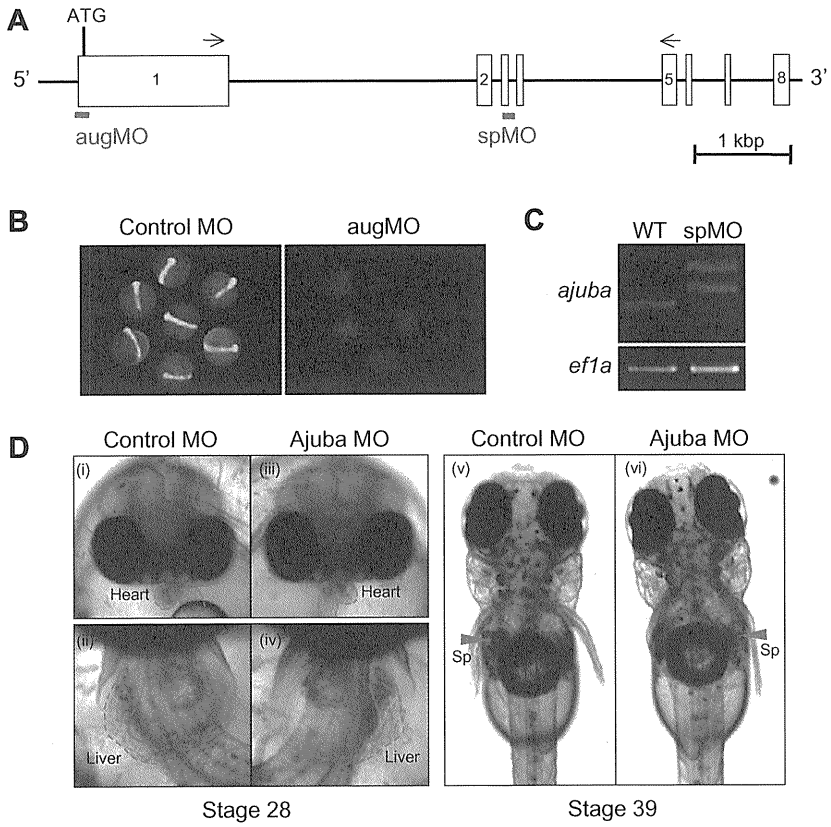

Fig. 2. Ajuba knockdown embryos show inverted positioning of the heart, liver and spleen. (A) Schematic diagram of exons 1–8 of the medaka *ajuba* genomic region. Arrows, positions of primer pairs used for the RT-PCR analysis in (C) below. augMO, translation-blocking morpholino; spMO, splice-blocking morpholino. (B) Validation of augMO. The cytoplasm of one-cell stage WT medaka embryos was co-injected with either control MO or augMO plus a GFP reporter gene that carries the Ajuba augMO target sequence at the 5′ UTR. Injection of augMO successfully blocked the translation of the GFP reporter protein. (C) Validation of spMO. WT medaka embryos were left untreated (WT) or injected with spMO, and RT-PCR was performed on total RNA. The *ajuba* RT-PCR product generated from RNA from spMO-injected embryos was increased in size compared to the control, reflecting the retention of intron sequences in the mature mRNA. Injection of spMO successfully interfered with the splicing of *ajuba* mRNA. (D) Laterality defects of organs in Ajuba morphants. In control morphants at stage 28, the heart tube jogged to the left and looped to the right (i) and the internal organs, including the liver, were located on the left side of midline (ii). In stage 28 Ajuba morphants, the heart tube jogged to the right and looped to the left (iii), and the position of the liver was reversed (iv). In stage 39 hatched larvae, the spleen was positioned on the left side in the control (v) but on the right side in the Ajuba morphant (vi). Sp, spleen.

the efficacy of the Ajuba augMO, this morpholino was co-injected into the cytoplasm of one-cell stage medaka embryos with an EGFP reporter containing the augMO target sequence. Co-injection of Ajuba augMO significantly reduced the translation of the EGFP reporter protein compared to co-injection of a control MO (Fig. 2B). To evaluate the efficacy of the splice-blocking morpholino (spMO), RT-PCR was carried out on total RNA prepared from embryos injected with 6 ng Ajuba spMO. The amplicon produced from gene-specific primers that span *ajuba* exons 1–5 resulted in abnormally large bands of two sizes (Fig. 2C). Sequence analysis revealed that these PCR products retained introns 2 and 3, causing a frame shift and introducing termination codons after exons 2 and 3, respectively. These data confirm the abilities of Ajuba augMO and spMO to disrupt expression and/or the function of the Ajuba protein.

Embryos injected with either Ajuba-spMO or Ajuba-augMO showed no alterations to body shape or size but did display defects in visceral asymmetries (Fig. 2D). In control morphants at stage 28, the ventricle of the heart looped towards the right and the atrium looped towards the left, and the liver and pancreas lay on the left side of the midline. In contrast, left–right asymmetry in the heart and liver was reversed in 30–32% of Ajuba morphants (Table S2). A similar rate of reversal was observed in the position of the spleen in Ajuba morphants at stage 39. Indeed, Ajuba morphants exhibited complete inversion of the positions of the abdominal and thoracic organs, an event reminiscent of the human disorder *situs inversus*. These results reveal that Ajuba regulates the left–right asymmetry of organs during medaka development.

3.3. Ajuba morphants display ectopic expression of left–right determinant genes

To understand the abnormal laterality phenotype of Ajuba morphants at the molecular level, we analyzed the expression patterns of genes that are normally expressed only on the left side of the embryo. In control morphants at stage 21, the nodal-related gene *southpaw* (*spaw*) was expressed in the left lateral plate mesoderm (LPM) (Fig. 3A, top left). However, Ajuba morphants showed a randomization of *spaw* expression, with 43–52% showing normal left-sided *spaw* expression but the remainder exhibiting right-sided (24–36%) or bilateral (21–24%) *spaw* expression in the LPM (Fig. 3A, top right and Table S3). The bilateral expression of *spaw* in the tailbud was unaffected in these mutants. The expression of another left-sided marker gene, *pitx2*, was also altered in Ajuba morphants. Control morphants showed normal left-sided expression of *pitx2* in the left diencephalon and the left LPM (Fig. 3A, bottom left). However, this asymmetric gene expression pattern was once again randomized in Ajuba morphants, with 27–38% of mutants exhibiting ectopic expression of *pitx2* (Fig. 3A, bottom right).

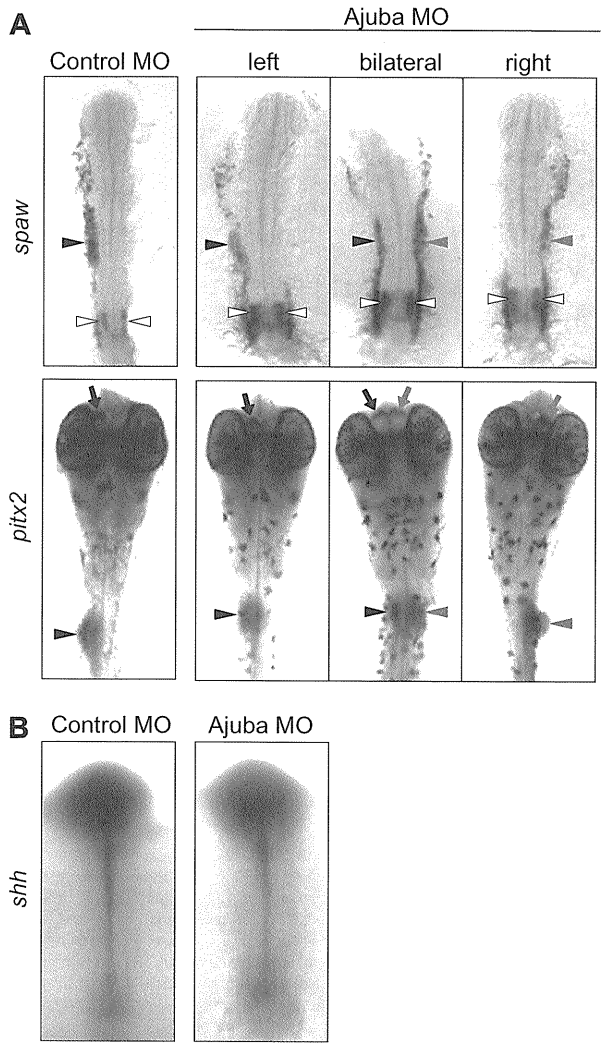

Fig. 3. Ajuba affects the expression of left-sided genes in the LPM and dorsal diencephalon. (A) Ectopic expression of *spaw* and *pitx2*. Control and *ajuba* morphants were analyzed by whole mount *in situ* hybridization to detect *spaw* expression at stage 21 (top) and *pitx2* expression at stage 26 (bottom). Dorsal views are shown. Top: *spaw* is normally expressed in the left LPM (black arrowheads). Altered bilateral or right expression of *spaw* (red arrowheads) appeared in Ajuba morphants. Normal bilateral expression of *spaw* at the KV (white arrowheads) was unaffected. Bottom: Left-sided expression of *pitx2* in control dorsal diencephalon (black arrows) was randomized (red arrows) in Ajuba morphants. (B) Normal expression of *shh* in the midline. Dorsal views of *shh* expression in control and Ajuba morphants are shown.

Because defects in embryonic midline integrity can lead to abnormal left–right development of internal organs [22], we compared the midline structure of control and Ajuba morphant embryos by examining *shh* expression via *in situ* hybridization. However, *shh* expression was not affected by the Ajuba knockdown (Fig. 3B), confirming that the midlines in these morphants were intact. These data demonstrate that Ajuba acts upstream of *spaw* and *pitx2* in the establishment of left–right asymmetry of the body plan.

3.4. Ajuba is essential for ciliogenesis of Kupffer's vesicle

One model for the establishment of the vertebrate left–right axis postulates the involvement of a ciliated organ known as the embryonic node in mice [2] or Kupffer's vesicle (KV) in zebrafish and medaka [23,24]. Motile cilia in the KV are thought to produce a leftward flow of extracellular fluid that induces the asymmetric expression of downstream genes such as *nodal* and *pitx2*. This model, combined with our observation of preferential expression of *ajuba* mRNA in cells surrounding the KV (Fig. 1C), prompted us to investigate the role of Ajuba in the development of ciliated cells in medaka. To determine if depletion of Ajuba caused defects in KV cilia, we subjected stage 21 Ajuba MO embryos to immunohistochemistry to detect acetylated tubulin, a major component of cilia. In contrast to control morphants, Ajuba augMO- or spMO-injected embryos developed shorter cilia (Fig. 4A). Quantification of ciliary lengths revealed a significant difference between control embryos and morphants (Fig. 4B), suggesting that KV cilia require Ajuba for normal development. In addition, the primary cilia of the telencephalon in Ajuba morphants were also shorter (Fig. S3).

The retina is another tissue heavily dependent on cilia, since photoreceptor cells have a highly specialized primary cilium called the outer segment (OS) that is essential for photoreception [25]. To determine whether loss of Ajuba affected retinal organization, we analyzed cross-sections of control and Ajuba morphant larvae but detected no alterations in OS or other components of photoreceptor cells in Ajuba morphants (Fig. 4C). Thus, Ajuba is required for normal ciliogenesis in some, but not all, cilium-dependent structures, most notably the KV governing left–right asymmetry.

4. Discussion

In this study, we cloned the medaka *ajuba* gene and discovered new roles for the Ajuba protein in early developmental processes. We have demonstrated that knockdown of Ajuba by antisense morpholinos disrupts the positions of the visceral organs and induces abnormal expression of genes involved in early left–right axis determination. In particular, Ajuba knockdown embryos showed shortened cilia lengths in the KV. Our results suggest a model in which Ajuba regulates left–right asymmetry by supporting the normal assembly of cilia in the KV.

Our subcellular localization studies showed that the Ajuba protein was present on basal bodies, which are ciliary initiators derived from centrosomes [4,5]. Another protein located on both the centrosome and the basal body is EB1, which is a microtubule-associated protein involved in mitosis and ciliogenesis [26]. A recent study has revealed that Ajuba is also associated with microtubules and may be important to ensure proper chromosome segregation [13]. Taken together, these observations suggest that Ajuba's function in ciliogenesis may depend on its ability to associate with microtubules. Studies are under way to address this issue.

The LIM domain has been identified in a highly diverse group of proteins [21]. We performed a phylogenetic analysis revealing that medaka express three closely related LIM proteins, Ajuba, Limd1 and Wtip, which are clustered with the three corresponding mammalian subfamily members (Fig. 1A). In contrast, *Xenopus* and *Drosophila* have no Ajuba homolog. *Xenopus* does have two homologs of Limd1 and Wtip, but *Drosophila* has only one homolog called CG11063 that belongs to the Wtip/Limd1 subfamilies. Recent studies have demonstrated that *Xenopus* Limd1 and Wtip are essential for epithelial-mesenchymal transitions in the neural crest during early development [27]. In addition, *Drosophila* CG11063 has been shown to negatively regulate the Hippo intracellular signaling pathway that controls cell survival and proliferation in the epithelial organs [28]. In our study, Ajuba-deficient medaka embryos displayed apparently normal development of the neural crest and epithelial organs (data not shown), implying that the functions of members of the Ajuba and Wtip/Limd1 subfamilies may overlap during early development. Pratt et al. have reported that Ajuba null mice are viable and reach adulthood without any obvious

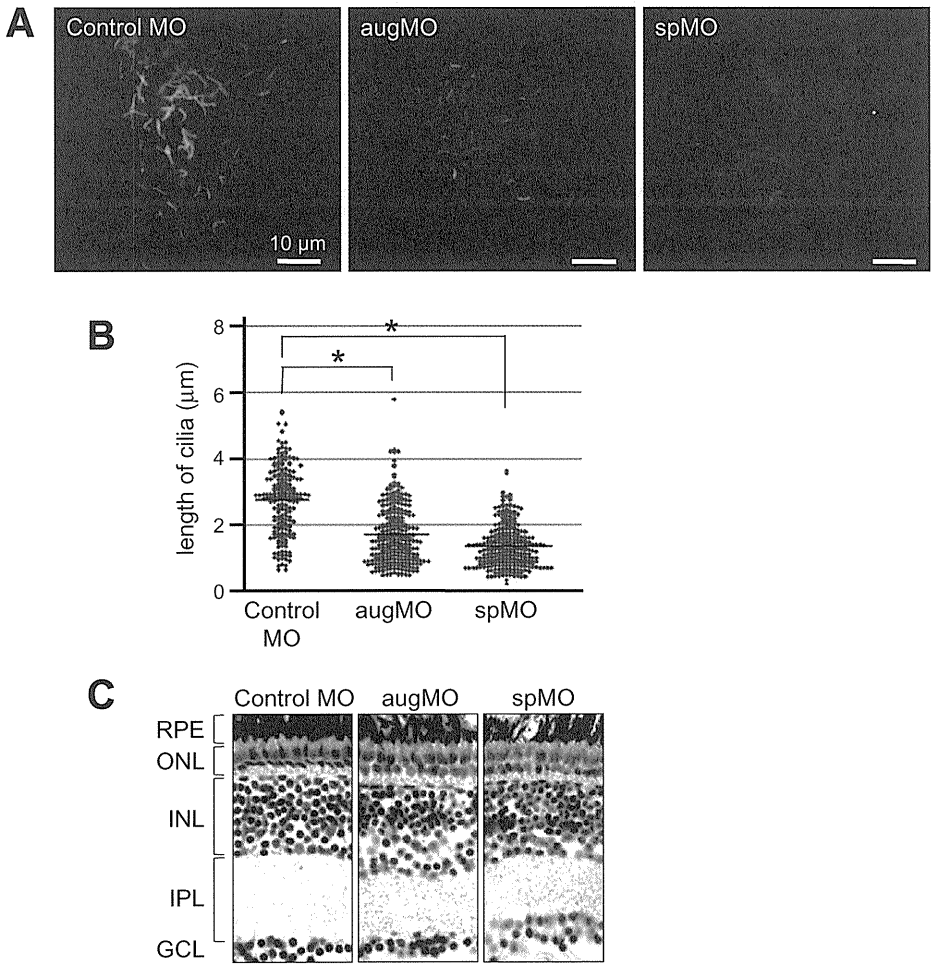

Fig. 4. Ajuba knockdown decreases ciliary length in the Kupffer's vesicle. (A) Defective cilia outgrowth but normal KV development. Stage 21 control, augMO and spMO morphant embryos were immunostained with anti-acetylated tubulin to visualize KV cilia. Whole-mount fluorescent images are shown. Cilia appear shorter in the absence of Ajuba. (B) Quantitation of decreased ciliary length. Lengths of primary cilia in the KV of the embryos in (A) were quantified using Image Browser software. Mean absolute cilium length was 2.78 μm for control embryos ($n = 197$ cilia), 1.72 μm for augMO morphants ($n = 224$ cilia), and 1.37 μm for spMO morphants ($n = 260$ cilia). $^{*}P < 0.01$. Horizontal line, mean. (C) Normal retinal structure. Transverse sections of the eyes of hatched control MO-, spMO- or augMO-injected embryos were stained with hematoxylin/eosin. There were no obvious structural defects in the retinas of Ajuba morphants. RPE, retinal pigment epithelium; ONL, outer nuclear layer (photoreceptor nuclei); INL, inner nuclear layer; IPL, inner plexiform layer; GCL, ganglion cell layer.

developmental pathologies [11]. A recent functional genomic screen using siRNA technology revealed that several dozen proteins are critical for the human ciliogenesis, but human Ajuba did not hit in the screen [29]. In Ajuba null medaka embryos, however, although the visceral organs develop normally, they are abnormally positioned in the body cavity (Fig. 2D). Precisely why Ajuba deficiency produced no significant abnormal phenotype in mice is not known. It may be that other unknown molecule(s) that do not exist in medaka serve redundant functions in the regulation of mammalian ciliogenesis. This discrepancy between the mammalian and medaka models highlights the dangers of relying on one system to define the function of a given gene, and further validates the use of our medaka knockdown system to explore the developmental roles of vertebrate gene families.

Acknowledgments

This work was supported in part by research grants from the Ministry of Education, Culture, Sports, Science and Technology (MEXT) of Japan, and the Japan Society for the Promotion of Science (JSPS). We are grateful to numerous members of the Nishina and Katada laboratories for critical reading and helpful discussions.

Appendix A. Supplementary data

Supplementary data associated with this article can be found, in the online version, at doi:10.1016/j.bbrc.2010.05.017.

References

[1] J.M. Gerdes, E.E. Davis, N. Katsanis, The vertebrate primary cilium in development, homeostasis, and disease, Cell 137 (2009) 32–45.
[2] N. Hirokawa, Y. Tanaka, Y. Okada, et al., Nodal flow and the generation of left–right asymmetry, Cell 125 (2006) 33–45.
[3] M. Fliegauf, T. Benzing, H. Omran, When cilia go bad: cilia defects and ciliopathies, Nat. Rev. Mol. Cell Biol. 8 (2007) 880–893.
[4] N. Santos, J.F. Reiter, Building it up and taking it down: the regulation of vertebrate ciliogenesis, Dev. Dyn. 237 (2008) 1972–1981.
[5] L.B. Pedersen, I.R. Veland, J.M. Schroder, et al., Assembly of primary cilia, Dev. Dyn. 237 (2008) 1993–2006.
[6] C.J. Wilkinson, M. Carl, W.A. Harris, Cep70 and Cep131 contribute to ciliogenesis in zebrafish embryos, BMC Cell Biol. 10 (2009) 17.

[7] E.A. Nigg, J.W. Raff, Centrioles, centrosomes, and cilia in health and disease, Cell 139 (2009) 663–678.
[8] R.K. Goyal, P. Lin, J. Kanungo, et al., Ajuba, a novel LIM protein, interacts with Grb2, augments mitogen-activated protein kinase activity in fibroblasts, and promotes meiotic maturation of Xenopus oocytes in a Grb2- and Ras-dependent manner, Mol. Cell. Biol. 19 (1999) 4379–4389.
[9] J. Kanungo, S.J. Pratt, H. Marie, et al., Ajuba, a cytosolic LIM protein, shuttles into the nucleus and affects embryonal cell proliferation and fate decisions, Mol. Biol. Cell 11 (2000) 3299–3313.
[10] H. Marie, S.J. Pratt, M. Betson, et al., The LIM protein Ajuba is recruited to cadherin-dependent cell junctions through an association with alpha-catenin, J. Biol. Chem. 278 (2003) 1220–1228.
[11] S.J. Pratt, H. Epple, M. Ward, et al., The LIM protein Ajuba influences p130Cas localization and Rac1 activity during cell migration, J. Cell Biol. 168 (2005) 813–824.
[12] M. Kisseleva, Y. Feng, M. Ward, et al., The LIM protein Ajuba regulates phosphatidylinositol 4,5-bisphosphate levels in migrating cells through an interaction with and activation of PIPKI alpha, Mol. Cell. Biol. 25 (2005) 3956–3966.
[13] A. Ferrand, V. Chevrier, J.P. Chauvin, et al., Ajuba: a new microtubule-associated protein that interacts with BUBR1 and Aurora B at kinetochores in metaphase, Biol. Cell 101 (2009) 221–235.
[14] Y. Abe, M. Ohsugi, K. Haraguchi, et al., LATS2-Ajuba complex regulates gamma-tubulin recruitment to centrosomes and spindle organization during mitosis, FEBS Lett. 580 (2006) 782–788.
[15] T. Hirota, N. Kunitoku, T. Sasayama, et al., Aurora-A and an interacting activator, the LIM protein Ajuba, are required for mitotic commitment in human cells, Cell 114 (2003) 585–598.
[16] T. Negishi, Y. Nagai, Y. Asaoka, et al., Retinoic acid signaling positively regulates liver specification by inducing wnt2bb gene expression in medaka, Hepatology 51 (2010) 1037–1045.
[17] M. Furutani-Seiki, T. Sasado, C. Morinaga, et al., A systematic genome-wide screen for mutations affecting organogenesis in Medaka, Oryzias latipes, Mech. Dev. 121 (2004) 647–658.
[18] D. Soroldoni, B. Bajoghli, N. Aghaallaei, et al., Dynamic expression pattern of Nodal-related genes during left–right development in medaka, Gene Expr. Patterns 7 (2007) 93–101.
[19] D. Kitagawa, T. Watanabe, K. Saito, et al., Genetic dissection of the formation of the forebrain in Medaka, Oryzias latipes, Mech. Dev. 121 (2004) 673–685.
[20] H. Mitani, N. Egami, Long term cultivation of medaka (Oryzias latipes) cells from liver tumors induced by diethylnitrosoamine, J. Fac. Sci., Univ. Tokyo, IV 14 (1980) 391–398.
[21] Q. Zheng, Y. Zhao, The diverse biofunctions of LIM domain proteins: determined by subcellular localization and protein–protein interaction, Biol. Cell 99 (2007) 489–502.
[22] B.W. Bisgrove, J.J. Essner, H.J. Yost, Multiple pathways in the midline regulate concordant brain, heart and gut left–right asymmetry, Development 127 (2000) 3567–3579.
[23] M. Hojo, S. Takashima, D. Kobayashi, et al., Right-elevated expression of charon is regulated by fluid flow in medaka Kupffer's vesicle, Dev. Growth Differ. 49 (2007) 395–405.
[24] J.J. Essner, J.D. Amack, M.K. Nyholm, et al., Kupffer's vesicle is a ciliated organ of asymmetry in the zebrafish embryo that initiates left–right development of the brain, heart and gut, Development 132 (2005) 1247–1260.
[25] V. Ramamurthy, M. Cayouette, Development and disease of the photoreceptor cilium, Clin. Genet. 76 (2009) 137–145.
[26] L.B. Pedersen, S. Geimer, R.D. Sloboda, et al., The Microtubule plus end-tracking protein EB1 is localized to the flagellar tip and basal bodies in Chlamydomonas reinhardtii, Curr. Biol. 13 (2003) 1969–1974.
[27] E.M. Langer, Y. Feng, H. Zhaoyuan, et al., Ajuba LIM proteins are snail/slug corepressors required for neural crest development in Xenopus, Dev. Cell 14 (2008) 424–436.
[28] M. Das Thakur, Y. Feng, R. Jagannathan, et al., Ajuba LIM proteins are negative regulators of the hippo signaling pathway, Curr. Biol. 20 (2010) 657–662.
[29] J. Kim, J.E. Lee, S. Heynen-Genel, et al., Functional genomic screen for modulators of ciliogenesis and cilium length, Nature 464 (2010) 1048–1052.

ARTICLE
Journal of Cellular Biochemistry 110:1022–1037 (2010)

Journal of Cellular Biochemistry

Negative Regulation of *wnt11* Expression by Jnk Signaling During Zebrafish Gastrulation

Jungwon Seo,[1,2] Yoichi Asaoka,[1*] Yoko Nagai,[1,2] Jun Hirayama,[3] Tokiwa Yamasaki,[1,2] Misako Namae,[1] Shinya Ohata,[1,2] Nao Shimizu,[1,2] Takahiro Negishi,[1] Daiju Kitagawa,[1] Hisato Kondoh,[4,5] Makoto Furutani-Seiki,[4,6] Josef M. Penninger,[7] Toshiaki Katada,[2] and Hiroshi Nishina[1*]

[1]*Department of Developmental and Regenerative Biology, Medical Research Institute, Tokyo Medical and Dental University, Tokyo 113-8510, Japan*

[2]*Department of Physiological Chemistry, Graduate School of Pharmaceutical Sciences, University of Tokyo, Tokyo 113-0033, Japan*

[3]*Medical Top Track Program, Medical Research Institute, Tokyo Medical and Dental University, Tokyo 113-8510, Japan*

[4]*SORST, Kondoh Differentiation Signaling Project, Japan Science and Technology Corporation, Kyoto 606-8305, Japan*

[5]*Graduate School of Frontier Biosciences, Osaka University, Osaka 565-0871, Japan*

[6]*Centre for Regenerative Medicine, Department of Biology and Biochemistry, University of Bath, Claverton Down, Bath BA2 7AY, UK*

[7]*Institute of Molecular Biotechnology of the Austrian Academy of Sciences, Dr. Bohr-gasse 3, Vienna A-1030, Austria*

ABSTRACT

Stress-induced Sapk/Jnk signaling is involved in cell survival and apoptosis. Recent studies have increased our understanding of the physiological roles of Jnk signaling in embryonic development. However, still unclear is the precise function of Jnk signaling during gastrulation, a critical step in the establishment of the vertebrate body plan. Here we use morpholino-mediated knockdown of the zebrafish orthologs of the Jnk activators Mkk4 and Mkk7 to examine the effect of Jnk signaling abrogation on early vertebrate embryogenesis. Depletion of zebrafish Mkk4b led to abnormal convergent extension (CE) during gastrulation, whereas Mkk7 morphants exhibited defective somitogenesis. Surprisingly, Mkk4b morphants displayed marked upregulation of *wnt11*, which is the triggering ligand of CE and stimulates Jnk activation via the non-canonical Wnt pathway. Conversely, ectopic activation of Jnk signaling by overexpression of an active form of Mkk4b led to *wnt11* downregulation. Mosaic lineage tracing studies revealed that Mkk4b-Jnk signaling suppressed *wnt11* expression in a non-cell-autonomous manner. These findings provide the first evidence that *wnt11* itself is a downstream target of the Jnk cascade in the non-canonical Wnt pathway. Our work demonstrates that Jnk activation is indispensable for multiple steps during vertebrate body plan formation. Furthermore, non-canonical Wnt signaling may coordinate vertebrate CE movements by triggering Jnk activation that represses the expression of the CE-triggering ligand *wnt11*. J. Cell. Biochem. 110: 1022–1037, 2010.

KEY WORDS: JNK; MKK4; GASTRULATION; CONVERGENT EXTENSION; *WNT11*; ZEBRAFISH

Abbreviations used: CE, convergent extension; Jnk, c-Jun N-terminal kinase; Mkk, mitogen-activated protein kinase kinase; Dpp, decapentaplegic; MO, morpholino; aa, amino acid; hpf, hours post-fertilization; WT, wild type; slb, silberblick; ppt, pipetail; caMkk4b, constitutively active Mkk4b.Jungwon Seo and Yoichi Asaoka contributed equally to this work.

Additional Supporting Information may be found in the online version of this article.

Grant sponsor: Scientific Research on a Priority Area from the Ministry of Education, Culture, Sports, Science and Technology of Japan; Grant sponsor: The Japan Society for the Promotion of Science, The Ministry of Education, Culture, Sports, Science and Technology of Japan; Grant sponsor: The Ministry of Health, Labor and Welfare of Japan.

*Correspondence to: Dr. Yoichi Asaoka, PhD and Dr. Hiroshi Nishina, PhD, 1-5-45 Yushima, Bunkyo-ku, Tokyo 113-8510, Japan.
E-mail: y-asaoka.dbio@mri.tmd.ac.jp, nishina.dbio@mri.tmd.ac.jp

Received 20 November 2009; Accepted 15 March 2010 • DOI 10.1002/jcb.22616 • © 2010 Wiley-Liss, Inc.
Published online 28 April 2010 in Wiley InterScience (www.interscience.wiley.com).

Stress-activated protein kinase/c-Jun N-terminal kinase (Sapk/Jnk) is activated in response to a variety of cellular stresses. Once activated, Jnk phosphorylates downstream targets, including the c-Jun component of the activator protein-1 (AP1) transcription factor. Mkk4 and Mkk7 are two upstream Mapk kinases that interact with downstream kinases and scaffold proteins to activate Jnk. The outcome of the signaling cascades initiated by Mkk4 and Mkk7 is the phosphorylation of the Tyr and Thr residues, respectively, in the Jnk's Thr-Pro-Tyr motif [Davis, 2000; Chang and Karin, 2001]. However, there is evidence that the specific transmission of signals from these upstream kinases to Jnk may rely on different sets of, and/or interactions with, downstream kinases and scaffold proteins [Whitmarsh et al., 1998], such that Mkk4 and Mkk7 have distinct biological functions in vivo. For example, Mkk7 (but not Mkk4) is an essential and specific component of the Jnk signaling pathway activated by proinflammatory cytokines [Tournier et al., 2001]. In addition, although they both die of massive liver cell apoptosis, $mkk4^{-/-}$ mice die on embryonic day 10.5 (E10.5), whereas $mkk7^{-/-}$ mice die on E11.5 [Nishina et al., 1997, 1999; Yang et al., 1997; Ganiatsas et al., 1998; Watanabe et al., 2002; Wada et al., 2004].

Analyses of various *jnk* knockout mice have revealed much about the physiological role of Jnk signaling in embryogenesis. In mammals, the Jnk family consists of three related genes, *jnk1*, *jnk2*, and *jnk3* [Derijard et al., 1994; Kallunki et al., 1994; Mohit et al., 1995]. A role for Jnk in tissue morphogenesis was first suggested by the observation that $Jnk1^{-/-}Jnk2^{-/-}$ double mutant mice died at E11 with defective closure of the neural tube in the hindbrain [Kuan et al., 1999]. In this case, Jnk was required to control the survival and apoptosis of neuronal cells. More recently, Jnk has emerged as a critical regulator of cell migration and the morphogenetic movement of epithelial sheets. In *Drosophila*, a well-orchestrated Jnk signaling pathway is required for the sealing of embryonic epidermis in a process known as dorsal closure [Glise et al., 1995; Riesgo-Escovar et al., 1996; Sluss et al., 1996]. Jnk is activated in the leading edge of the dorsal epidermis at the onset of dorsal closure and drives the expression of the TGFβ homolog Decapentaplegic (Dpp), a secreted morphogen that regulates dorsal closure [Reed et al., 2001]. Little is known as yet about the function of the Jnk pathway in vertebrate morphogenesis, particularly when the body plan is first laid down.

The basic body plan of vertebrate embryos is established during gastrulation by a series of coordinated cell movements that lead to the formation of endoderm, mesoderm, and ectoderm, and overtly shape the embryonic axis [Keller, 2002]. A major driving force of vertebrate gastrulation is convergent extension (CE), a mechanism in which dorsal mesodermal cells polarize, elongate along the mediolateral axis, and intercalate toward the midline (convergence), leading to the extension of the anterior–posterior axis of the embryo [Keller, 2002; Tada et al., 2002; Seifert and Mlodzik, 2007]. CE is well conserved among vertebrate species, including in frog (*Xenopus laevis*) and zebrafish (*Danio rerio*) [Solnica-Krezel, 2005].

The study of gastrulation in mammals is difficult because these animals develop in utero, preventing direct observation of the embryos. In contrast, fertilized zebrafish eggs develop ex utero into transparent embryos that can be directly observed and are highly amenable to manipulations such as tissue transplantation and molecular perturbation. There is a high degree of conservation between zebrafish and mammalian genes, and a shared developmental path that results in fundamental similarities in many tissues and organs. In addition, there exists a wide selection of mutant zebrafish lines with developmental abnormalities, including gastrulation defects. Thus, zebrafish provide a very attractive alternative to mammals for studying the molecular and cellular bases of vertebrate morphogenesis.

Genetic analyses of gastrulation mutants in zebrafish and functional studies in *Xenopus* have revealed that CE is regulated by the non-canonical Wnt signaling pathway, which does not involve β-catenin [Seifert and Mlodzik, 2007]. Wnt11 and Wnt5 have been found to be essential ligands for normal cell movements during vertebrate CE. The zebrafish mutants *silberblick* (*slb*) and *pipetail* (*ppt*) have a mutation in *wnt11* or *wnt5*, respectively, and *slb–ppt* double mutants show severe CE defects [Heisenberg et al., 2000; Kilian et al., 2003]. Interestingly, *wnt5* mRNA can partially rescue the *slb* phenotype [Kilian et al., 2003], indicating a partial redundancy of Wnt11 and Wnt5 functions. In *Xenopus*, Wnt11 and Wnt5 bind to the Frizzled receptor, initiating non-canonical Wnt signaling that leads to activation of RhoA and Rac [Habas et al., 2001, 2003]. This RhoA and Rac activation triggers Jnk signaling critical for CE in *Xenopus* [Habas et al., 2003; Kim and Han, 2005]. Notably, depletion of Jnk in *Xenopus* causes defective gastrulation in these animals [Yamanaka et al., 2002]. All these findings suggest that Jnk is an essential component of the non-canonical Wnt pathway involved in vertebrate CE. However, the precise molecular mechanism by which Jnk signaling regulates CE has remained obscure. In an effort to elucidate the downstream targets of Jnk signaling in the non-canonical Wnt pathway that is associated with early embryogenesis, we have analyzed the functions of Mkk4 and Mkk7 orthologs in zebrafish (Mkk4a, Mkk4b, and Mkk7). Using morpholino-mediated knockdown, we demonstrate that Mkk4b is essential for CE movements. Furthermore, we provide the first evidence that *wnt11* itself is a downstream target of the Jnk cascade in the non-canonical Wnt pathway associated with early embryogenesis.

MATERIALS AND METHODS

ZEBRAFISH STRAINS

The AB and TL wild-type (WT) strains were maintained essentially as described in "The Zebrafish Book" [Westerfield, 1994]. Embryos were produced by natural matings and staged by standard morphological criteria or by hours post-fertilization (hpf), as described [Kimmel et al., 1995; Asaoka et al., 2002].

CLONING OF ZEBRAFISH MKK4 AND MKK7 GENES

Zebrafish sequences highly homologous to mouse *mkk4* and *mkk7* cDNAs were identified by database searching. Full-length zebrafish cDNAs were obtained by 5′- and 3′-RACE PCR according to the manufacturer's protocols (Invitrogen). RACE-PCR fragments were purified and subcloned into pGEM-T easy (Promega).

SEMI-QUANTITATIVE RT-PCR ANALYSIS

Total RNA was isolated from embryos at various developmental stages using TRIzol reagent according to the manufacturer's

protocol (Invitrogen). First-strand cDNA was synthesized from 1 μg total RNA using SuperscriptIII reverse transcriptase (Invitrogen) and a random or oligo-dT primer. Semi-quantitative PCR was done essentially as described [Okuda et al., 2006]. Primers used for RT-PCR analysis of mRNA expression in zebrafish extracts were as follows: for *mkk4a*, 5′-CGTTC AACAG TAGAC GAGCG-3′ and 5′-AATCA CTTCG TCTAA AGAGG-3′; for *mkk4b*, 5′-CGCTC CACGG TGGAT GAGAA-3′ and 5′-AATGA CGTCA TCTGA CGCAC-3′; for *mkk7*, 5′-TGGCC ATGTC ATCGC AGTCA-3′ and 5′-GGAAA CTGTC CTGTG GCTAG-3′; for *β-actin*, 5′-CAGCT TCACC ACCAC AGC-3′ and 5′-GTGGA TACCG CAAGA TTCC-3′; for *jnk1a-1*, 5′-AGCGT ATGAC CACGT CCTCG-3′ and 5′-GGGCC AGACC GAAAT CCAG-3′; for *jnk1a-2*, 5′-GGATG CTTAC ACATC GACTT CAC-3′ and 5′-CATCC ATCAG CTCCA TTACT AGG-3′; for *jnk2*, 5′-ATCTG GACCA TGAGA GGATG TC-3′ and 5′-CTGGG GTTTG TTCAT CACAT AG-3′; for *e-cadherin*, 5′-ACAAA CTTAG GGCTC ATGCG-3′ and 5′-ACAGA TGCAG TGTAC GAGGA-3′; for *stat3*, 5′-TGAAT GGAAA CAGCC AGGCA-3′ and 5′-TTTGA TGACA AGGGG TCGGT-3′; for *liv1*, 5′-CGGTT GCCAA TATGA TTGGC-3′ and 5′-GGTGG ATTCC TGGTT CATCT-3′; for *wnt5*, 5′-CCGGA GATGT ACATC ATTGG-3′ and 5′-TTCTC ACGTT CACGA GCGTC-3′; for *wnt11*, 5′-GTAAA CTTCT GGACG GGCTC-3′ and 5′-CGAAG GTTAT CTCCA CATCC-3′.

ZEBRAFISH EMBRYO PREPARATION

Embryos were deyolked with deyolking buffer (1/2 Ginzburg Fish Ringer) without calcium [Link et al., 2006]. Subsequently embryos were lysed in buffer containing 100 mM NaCl, 40 mM Tris-HCl (pH 8.0), 1% Nonidet P-40, 0.05% 2-mercaptoethanol, 1 mM EDTA, 1 mM EGTA, 4 μg/ml aprotinin, 100 μM Na_3VO_4, and 50 mM NaF, and sonicated for 1 min. Lysates were centrifuged at 20,000*g* to pellet cellular debris. Protein concentration was measured by BCA™ Protein Assay Kit (Pierce).

ES CELL LINES

Mkk4$^{-/-}$ and *mkk7*$^{-/-}$ murine ES cell lines were generated as previously described [Nishina et al., 1997; Fleming et al., 2000; Kishimoto et al., 2003].

ANTIBODIES

Anti-Jnk1 polyclonal Ab (FL), which recognizes both the 46 and 55 kDa splice variants of Jnk1, was from Santa Cruz Biotechnology, Inc. Anti-phospho-Jnk (9251) and anti-FLAG (M2) Abs were from Cell Signaling Technology and Sigma-Aldrich Co., respectively.

CONSTRUCTION OF PLASMIDS AND TRANSFECTION

cDNAs encoding FLAG-tagged zebrafish Mkk4a-l, Mkk4b, and Mkk7 were cloned into the mammalian expression vector pCE-IRES2-EGFP [Ura et al., 2007]. ES cells were plated at 1×10^6 cells/35-mm dish and transfected 1 day later with expression construct (4 μg) plus Lipofectamine 2000 reagent (Invitrogen). Transfected cells were stimulated with UV light (1 kJ/m^2) and subjected to standard Western blot analysis as described below.

WESTERN BLOT ANALYSIS

Proteins were fractionated by SDS-PAGE and transferred to a polyvinylidene difluoride membrane that was then incubated for 1 h in blocking solution (2% or 5% skim milk in Tris-buffered saline [TBS]). The blocked membrane was incubated for 1 h in blocking solution containing anti-phospho-Jnk, anti-Jnk1, or anti-FLAG Ab. The membrane was then washed in TBS-Tween 20 (0.05%), incubated with anti-mouse/rabbit horseradish peroxidase-conjugated Ab (Jackson ImmunoResearch Laboratory) for 30 min, and washed three times in TBS-Tween 20. Proteins were visualized using Immobilon HRP (Millipore) or the SuperSignal West Femto Kit (Pierce) and a ChemiDoc XRS system (Bio-Rad), as described [Kishimoto et al., 2003].

ANTI-SENSE MORPHOLINO (MO) AND MRNA INJECTIONS

All MOs were designed to bind to exon-intron junctions and were synthesized by Gene Tools (Philomath, OR). Sequences of splice-blocking MOs were as follows: *mkk4a* MO, 5′-GATGA AACAG ACGAA CCTCT CTGAA-3′; *mkk4b* MO, 5′-TGTGT GTGTC TGACC TCTCT GAAGA-3′; *mkk7* MO, 5′-AGAGG AACTC ACCAG AGAAA TGCCA-3′; *jnk1a-1* MO, 5′-AGACA AATAA CTTAC ACATC CTGGA-3′; *jnk1a-2* MO, 5′-ATTTC AGTGT CTTGA CTTAC ATTTT-3′; *jnk2* MO, 5′-AAAAA CAGCA TTACC ATTCT CCTTG-3′. Sequences of translation-blocking MOs were: *mkk4a-l* atgMO, 5′-GCGTC GCCAT TTGGG TTTGA CTCTT-3′; *mkk4b* atgMO, 5′-AGAGT CACTG CTGGG AGCCG CCATT-3′; *mkk7* atgMO, 5′-AGAGT CTCTG CTCCA GCGAC GACAT-3′; *mkk4a-s* atgMO, 5′-GCCAT CTTGT TGACC GAGCC ATACG-3′. The standard control MO was: 5′-CCTCT TACCT CAGTT ACAAT TTATA-3′.

For knockdown, MO solution was injected into the yolks of one- to four-cell stage zebrafish embryos immediately beneath the cell body. For *wnt5* or *wnt11* overexpression, a construct designed to produce mRNA encoding full-length zebrafish *wnt5* or *wnt11* was created by cloning the relevant fragment (amplified by high-fidelity PCR) into the pCS2+ plasmid. A constitutively active form of Mkk4b (caMkk4b) was constructed by replacing Ser275 and Thr279 with aspartic acid and glutamic acid, respectively, and subcloning into the pCS2+ plasmid. Sense strand capped mRNA was synthesized using SP6 RNA polymerase and the mMESSAGE mMACHINE system (Ambion). RNA injections were performed as described [Shinya et al., 2000].

WHOLE-MOUNT IN SITU HYBRIDIZATION

Digoxigenin-labeled RNA probes were synthesized using the DIG RNA Labeling Kit (Roche Diagnostics). Primers used for mRNA expression analysis in whole zebrafish embryos were as follows: for *dlx3*, 5′-TCCGA CTTCT AAGGA CTCTC-3′ and 5′-TTCAC CTGTG TCTGT GTGAG-3′; for *ntl*, 5′-AGACG AATGT TTCCC GTGCT-3′ and 5′-CTTCT CTCTT TGGCA TCGAG-3′; for *hgg1*, 5′-ATGAG GAGTT CAGAC AGGCA-3′ and 5′-ATTAC CGCTG GGAAT GTCCA-3′; for *pax2.1*, 5′-CCGGC AGTAT TAAAC CTGGA-3′ and 5′-AGGTG CTTCC GTAAA CTCTC-3′; for *gsc*, 5′-GTCAC TATGA AGGAC ACTCG TGC-3′ and 5′-TTTGT TCCTG TTTTC AGGCG AC-3′; for *wnt5*, 5′-GTAGC AGACG TGAGC ACTGG-3′ and 5′-CGCAT TCCGA AAGTT CTTAA GAG-3′. Mixtures of three riboprobe pairs were used to detect *wnt11*, as follows: (1) 5′-GTAAA CTTCT GGACG GGCTC-3′ and 5′-CTAAA GTCCT GTGGG CCTGA-3′; (2) 5′-CCGGA ATTCA TGACA GAATA CAGGA ACT-3′ and 5′-CGAAG GTTAT CTCCA CATCC-3′; (3) 5′-GGTGC TTATG GACTC TCTAG-3′ and 5′-GAGTC GACTC

ACTTC GAGAC GTATC TCT-3′. Riboprobes for *myoD* and *krox20* were used as described [Shinya et al., 2000]. Whole mount in situ hybridization procedures were performed essentially as described [Thisse et al., 1993].

QUANTITATIVE REAL-TIME RT-PCR

Quantitative real-time RT-PCR analyses were performed using the Chromo4 real-time detection system (Bio-Rad). The PCR primers used were as follows: for *wnt11*, 5′-CACAA CAATG CTGTT GGCAG ACAGG TG-3′ and 5′-GGAGA TGGTG CTGAT GTCTT GAAGA CC-3′; for *β-actin*, 5′-GCAGA TGTGG ATCAG CAAGC AGG-3′ and 5′-CTGAG TCAAT GCGCC ATACA GAG-3′. For a 20 μl PCR reaction, cDNA template was mixed with 10 μl iQ SYBR Green Supermix (Bio-Rad) plus the appropriate primers to a final concentration of 200 nM each. The reaction was first incubated at 95°C for 3.5 min, followed by 41 cycles of 95°C for 12 s, 60°C for 13 s, and 72°C for 18 s.

RESULTS

CLONING AND CHARACTERIZATION OF ZEBRAFISH MKK4A, MKK4B, AND MKK7 GENES

To unravel the role of Jnk signaling in early zebrafish development, we first determined whether zebrafish *mkk4* and *mkk7* could function as direct activators of Jnk. We performed BLAST searches with mouse *mkk4* and *mkk7* to enable predictions of zebrafish *mkk4* and *mkk7* cDNA sequences. The obtained EST sequences were subjected to 5′- and 3′-RACE methodology to acquire the full-length cDNA sequences. The zebrafish has two *mkk4* genes, named *mkk4a* and *mkk4b* (GenBank accession no. AB438979), but only one *mkk7* ortholog (GenBank accession no. AB438980). The predicted amino acid (aa) sequences of the proteins encoded by these zebrafish genes are 81–84% identical to those of the mouse, and the Mkk phosphorylation sites are conserved (Fig. S1A). Two splice variants of zebrafish *mkk4a* were identified: *mkk4a-s* and *mkk4a-l* (GenBank accession nos. AB030901 and AB438978). Mkk4a-s (281 aa) is an N-terminal truncated form of Mkk4a-l (404 aa). A phylogenetic analysis of vertebrate *mkk4* genes revealed that zebrafish *mkk4a* was clustered with mammalian *mkk4* genes, whereas zebrafish *mkk4b* was clustered with those of other teleosts (Fig. S1B). These phylogenetic relationships suggest that the duplication of the *mkk4* gene occurred in the common ancestors of teleosts and tetrapods.

We next used semi-quantitative RT-PCR to examine the expression dynamics of *mkk4a*, *mkk4b*, and *mkk7* during early zebrafish development. All three genes were continuously expressed from the one-cell stage to the blastula (4.7 hpf) (Fig. 1A). Levels of both *mkk4a* and *mkk7* were markedly decreased by the shield stage and became relatively low at the tailbud stage. In contrast, *mkk4b* expression was essentially constant from the one-cell stage through to the shield stage and relatively high during later gastrula stages.

To monitor Jnk activity during zebrafish embryogenesis, we prepared protein extracts from zebrafish embryos collected at each of the 30% epiboly, shield, 75% epiboly, and tailbud stages, and examined the relative amounts of the active, phosphorylated form of Jnk by Western blot analysis. Jnk activity was detected from 30% epiboly and relatively high during later gastrula stages (Fig. 1B), suggesting the possibility that Jnk plays a role in the gastrulation stage.

In mammals, Mkk4 and Mkk7 have distinct biochemical properties and preferentially phosphorylate the Tyr and Thr residues, respectively, within the Thr-Pro-Tyr motif of Jnk [Lawler et al., 1998; Kishimoto et al., 2003]. To qualitatively determine whether these distinctions applied to the zebrafish orthologs of Mkk4 and Mkk7, and to gauge the functional relatedness of the mammalian and zebrafish enzymes, we analyzed whether zebrafish Mkks could compensate for the lack of mouse Mkk4 and Mkk7 in $mkk4^{-/-}$ and $mkk7^{-/-}$ murine ES cells, respectively. We transfected zebrafish *mkk4a-l*, *mkk4b*, and *mkk7* expression vectors separately into $mkk4^{-/-}$ or $mkk7^{-/-}$ ES cells, which lack the capacity to activate Jnk in response to UV irradiation [Nishitai et al., 2004]. We then subjected the transfected cells to UV irradiation and assessed Jnk activation. We found that zebrafish Mkk4a-l or Mkk4b, but not Mkk7, rescued UV-induced Jnk activation in $mkk4^{-/-}$ ES cells (Fig. 1C, lanes 2–4). Conversely, zebrafish Mkk7, but not Mkk4a-l or Mkk4b, rescued UV-induced Jnk activation in $mkk7^{-/-}$ ES cells (Fig. 1C, lanes 6–8). These results suggest that zebrafish Mkk4 and Mkk7 are analogous in function to their murine counterparts and play distinct biochemical roles during stress-induced Jnk activation.

ZEBRAFISH *MKK4B* IS INDISPENSABLE FOR NORMAL CE REGULATION

To elucidate the physiological roles of Mkk4a, Mkk4b, and Mkk7 during early zebrafish development, we performed anti-sense morpholino (MO)-mediated knockdown of each gene's mRNA and analyzed its residual expression by RT-PCR. Microinjection of *mkk4b* MO effectively prevented correct splicing of target pre-mRNA from the shield to tailbud stages (Fig. 2A). As a result, *mkk4b* morphants exhibited severe defects in anterior–posterior extension after gastrulation. At 11 hpf, *mkk4b* morphants displayed an MO dose-dependent shortening of body length (Fig. 2B, row 1) that did not recover at later developmental stages (Fig. 2B, rows 2 and 4). In addition, *mkk4b* morphants displayed broader notochords and somites during early segmentation than did control MO-injected embryos (Fig. 2B, row 3), indicating that CE is defective in the absence of Mkk4b. Quantification of the anterior–posterior axis extension and mediolateral convergence at 16 hpf revealed that *mkk4b* knockdown significantly increased the angle between the anterior and posterior ends of the embryo, as well as its mediolateral distance, in a MO dose-dependent manner (Fig. 2C).

With respect to marker expression patterns, *mkk4b* morphants showed a more posteriorly and broadly positioned prechordal plate (*hgg1*), a wider neural plate (*dlx3* and *pax2.1*), and a shorter and broader notochord (*ntl*) at the tailbud stage than did controls (Fig. 2D). Although their body axis was shorter and their somites wider, *mkk4b* morphants had the same numbers and shapes of rhombomeres (marked by *krox20* expression) and somites (*myoD*) as control embryos at the eight-somite stage (Fig. 2E), implying that Mkk4b has no obvious role in specifying cell fate.

To further confirm that it was loss of Mkk4b that was responsible for the observed CE defects, we co-injected *mkk4b*

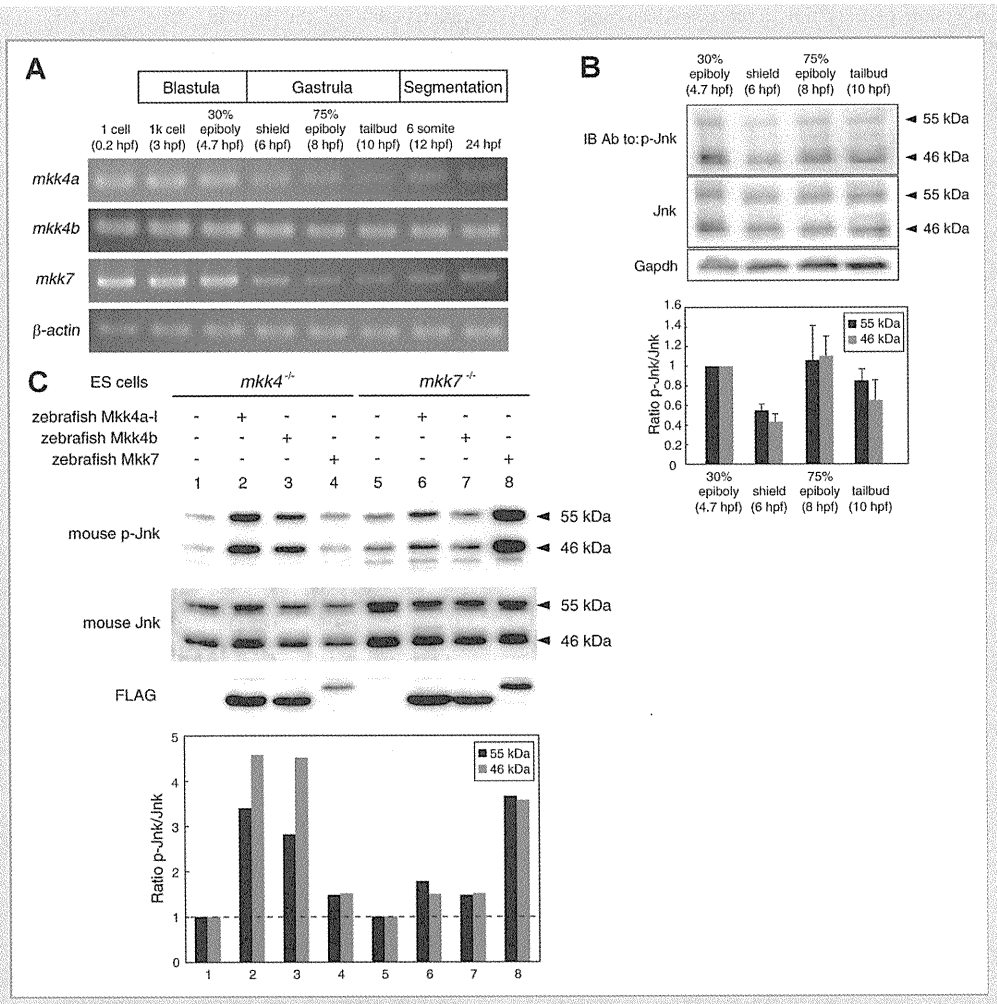

Fig. 1. Expression and biochemical properties of zebrafish *mkk4a*, *mkk4b*, and *mkk7* gene products during early development. A: Temporal expression patterns of zebrafish *mkks*. Semi-quantitative RT-PCR reveals relatively high expression of *mkk4b* up to 24 hpf in WT embryos, whereas *mkk4a* and *mkk7* levels abruptly decrease around the shield stage. Lanes 1–8 correspond to template cDNA derived from 0.2 to 24 hpf embryos (n = 30, 30, 50, 20, 20, 20, 30, 50 embryos, respectively). *β-Actin*, loading control. B: Analysis of Jnk activity during zebrafish embryogenesis. Approximately 50 μg of protein was loaded in SDS–PAGE in each lane. Activated Jnk and total Jnk were detected with anti-phospho-Jnk (p-Jnk) and anti-total-Jnk antibodies, respectively. Image shown is representative of three separate experiments with similar results (top). Graphic results are expressed as a ratio of p-Jnk to total Jnk and the value of 30% epiboly stage is assigned an arbitrary value of 1 (bottom). Data shown are the mean ± SEM of three independent experiments. C: Effects of zebrafish Mkk4 or Mkk7 expression on stress-induced Jnk activation in *mkk4* $^{-/-}$ or *mkk7* $^{-/-}$ mouse ES cells. *Mkk4* $^{-/-}$ or *mkk7* $^{-/-}$ mouse ES cells were transfected with zebrafish *mkk4a-l*, *mkk4b*, or *mkk7* expression vectors, cultured for 24 h, and stimulated with UV (1 kJ/m^2). Expression levels of zebrafish Mkks (FLAG) and endogenous levels of p-Jnk and total Jnk (46 and 55 kDa isoforms) in cell lysates were detected by Western blotting (top). The histogram shows quantitative representations of the relative activated Jnk, which was expressed as a ratio of p-Jnk to total Jnk (bottom). The values of lanes 1 and 5 are assigned an arbitrary value of 1.

MO with in vitro-transcribed *mkk4b* mRNA and assayed for the rescue of the CE defects. Inspection of live co-injected embryos showed that the synthetic *mkk4b* mRNA was able to prevent *mkk4b* MO-induced defects (Fig. S2). Thus, the observed phenotypes are the result of specific knockdown of Mkk4b by the *mkk4b* MO.

To rule out the possibility that the observed phenotypes in *mkk4b* knockdown embryos were secondary to a patterning alteration, we evaluated the distribution of *goosecoid* (*gsc*), a dorsal mesoderm "organizer" marker at the shield stage. No alterations to the *gsc* expression pattern were observed in *mkk4b* morphants (Fig. 2F), indicating that dorsoventral specification is not disturbed by *mkk4b* MO treatment.

The data in Figure 2D suggested that *mkk4b* morphants developed slightly slower than controls. To determine if Mkk4b influences epiboly, we monitored the development of live embryos over a time course of 6–10 hpf. As was true for control embryos, gastrulation began at 6 hpf in *mkk4b* morphants and 75% epiboly was reached at 8 hpf (Fig. S3). However, whereas control embryos had completed their epiboly movements by 10 hpf, *mkk4b* morphants exhibited a mild delay in epiboly that extended it to 11 hpf (Figs. S3 and 2B). Thus, Mkk4b activity is not required for the initiation or progression of epiboly but does influence its late phase.

When parallel experiments were used to examine the importance of Mkk4a in early zebrafish development, a very different result was

obtained. Microinjection of 0.8 pmol of *mkk4a* MO reduced WT *mkk4a* mRNA beginning at the shield stage (Fig. S4A). Unlike *mkk4b* morphants, however, *mkk4a* morphants had no gross morphological abnormalities (Fig. S4B), and the expression patterns of *hgg1*, *dlx3*, *ntl*, and *pax2.1* were completely normal (Fig. S4C).

In morphants injected with 0.8 pmol of *mkk7* MO, expression of the WT *mkk7* transcript declined by the shield stage and was undetectable at the tailbud stage (Fig. 2G). Instead, a shorter amplification product was detected. Like *mkk4b* morphants, *mkk7* morphants exhibited an MO dose-dependent shortening of body length at 24 hpf (Fig. 2H). However, the expression patterns of *hgg1*, *dlx3*, *ntl*, and *pax2.1* were normal in *mkk7* morphants, even at a high dose of MO (1.5 pmol) (Fig. 2I). These data suggest that *mkk7* is dispensable for proper gastrulation. Nevertheless, during

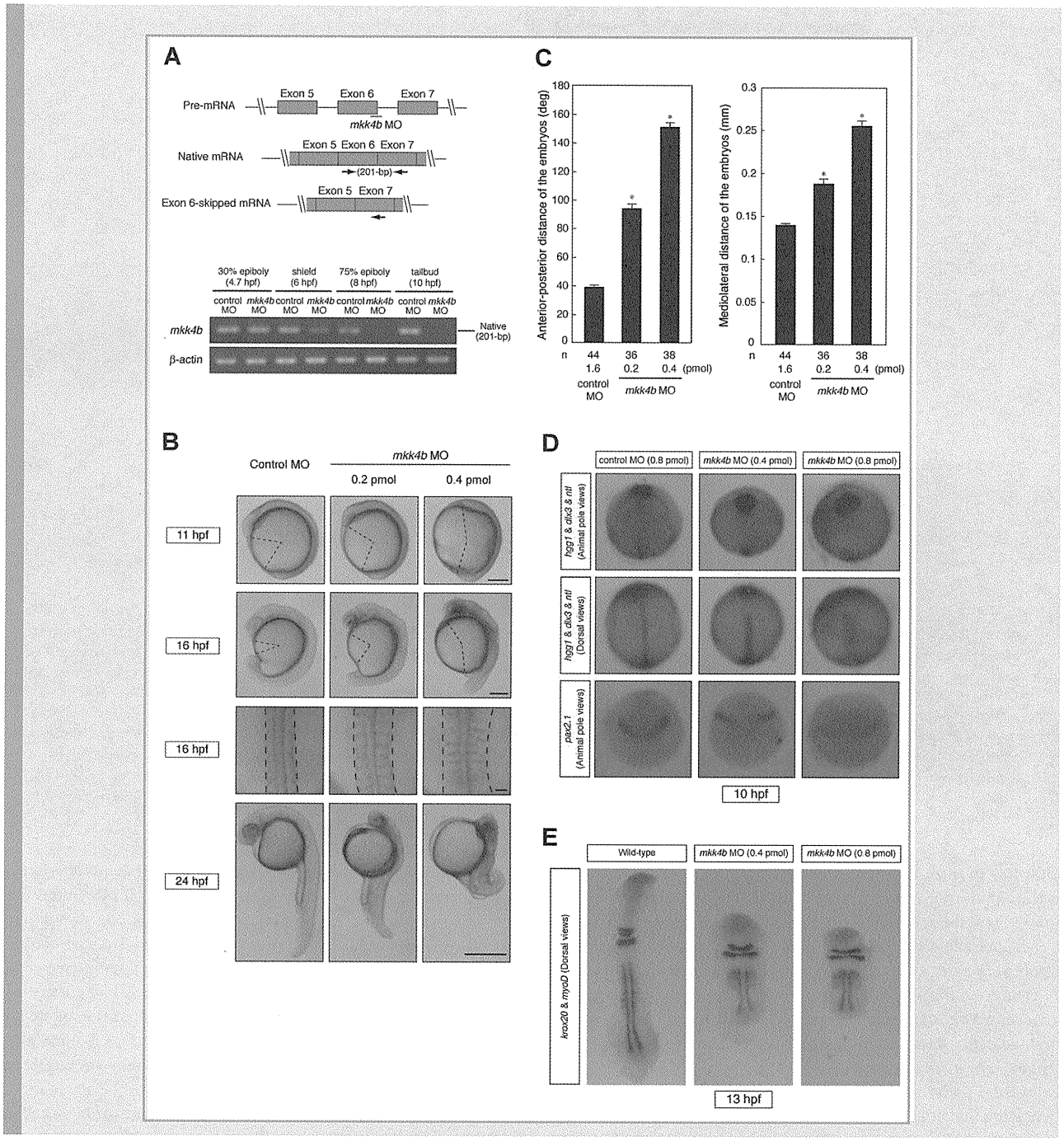

segmentation, the *mkk7* morphants displayed somites of abnormal patterning and morphology (Fig. 2J). Thus, Mkk7 function is essential for normal somite morphogenesis.

Because the *mkk4a*, *mkk4b*, and *mkk7* genes are maternally expressed, it was possible that their expression products might persist throughout gastrulation. To rule out this possibility, we used translation-blocking MOs (atgMOs) that would specifically target maternal and zygotic *mkk* transcripts and prevent their translation. We injected embryos with a specific translation-blocking MO (*mkk4a-l* atgMO, *mkk4b* atgMO, or *mkk7* atgMO) and examined their development using gross morphological analysis and in situ hybridization. By 23 hpf, *mkk4b* atgMO- or *mkk7* atgMO-injected embryos showed reduced body length compared to control-injected embryos, whereas few or no morphological differences were apparent in *mkk4a* atgMO-injected embryos (Fig. S5A). *Mkk4b* atgMO-injected embryos also showed altered expression of several marker genes (*hgg1*, *dlx3*, *ntl*, and *pax2.1*; Fig. S5B), highlighting the morphological abnormalities associated with defective CE movements at 10 hpf. This phenotype was strikingly similar to that of embryos subjected to *mkk4b* splice-blocking MO knockdown (Fig. 2D). Taken together, these results demonstrate that Mkk4b but not Mkk4a is essential for co-ordinated CE. In the following analyses, we focused on the specific role of Mkk4b–Jnk signaling in proper CE movements during gastrulation.

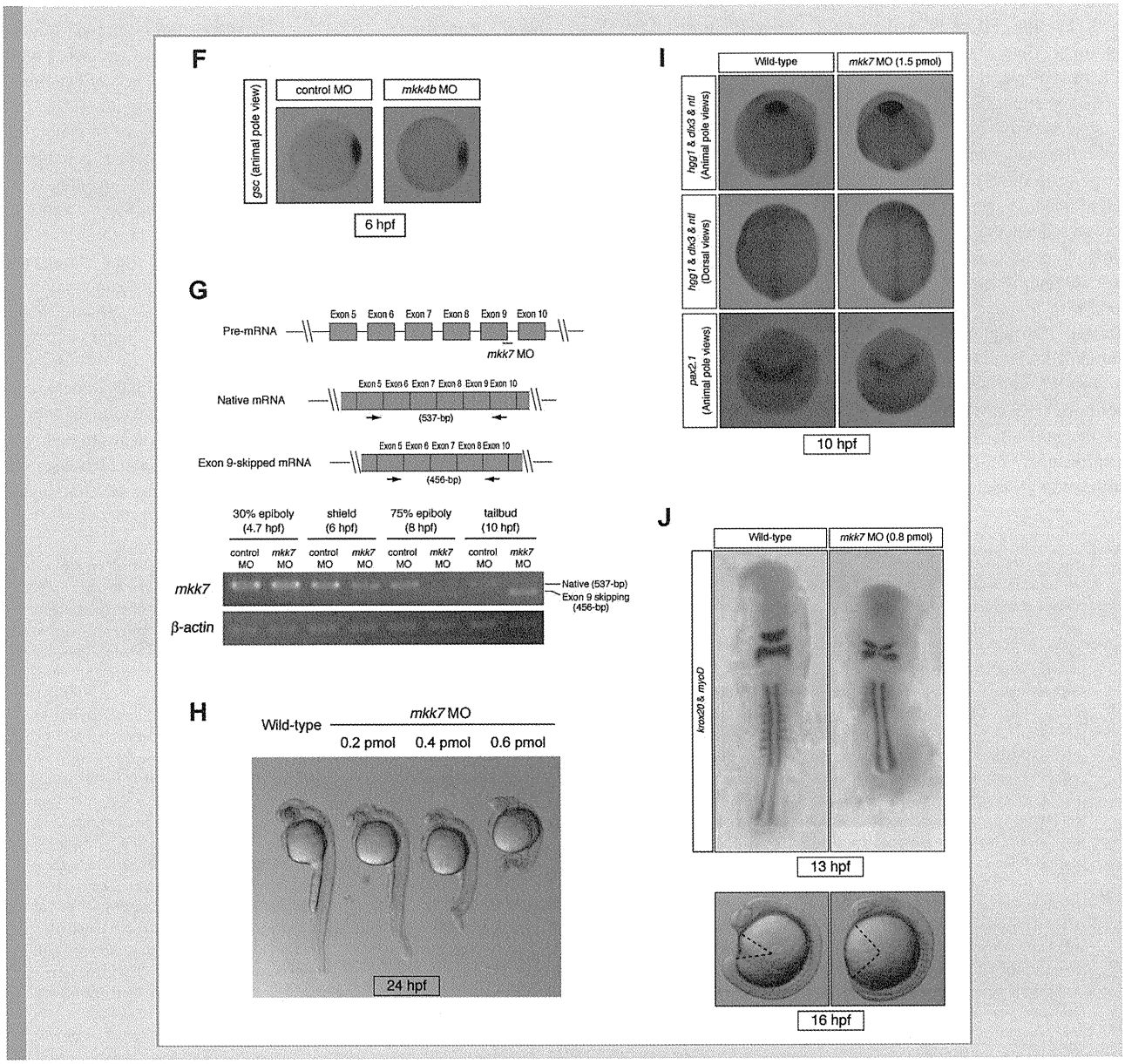

ZEBRAFISH JNK2 IS NECESSARY FOR CORRECT CE MOVEMENTS

It has previously been reported that non-canonical Wnt signaling regulates CE movements in *Xenopus* through the activation of Jnk [Yamanaka et al., 2002]. We therefore asked whether overexpression of *wnt11* or *wnt5* could activate Jnk during zebrafish gastrulation. Extracts from zebrafish embryos overexpressing *wnt11* or *wnt5* mRNA were prepared at 75% epiboly (8 hpf) and subjected to Western blotting with anti-phospho-Jnk antibody. This analysis confirmed that *wnt11* or *wnt5* overexpression significantly increased levels of the active, phosphorylated form of Jnk (Fig. 3A). Furthermore, analysis of extracts from embryos injected with 0.4 pmol *mkk4a* MO, *mkk4b* MO, or *mkk7* MO showed that Jnk phosphorylation was significantly decreased in *mkk4b* morphants but still detected in *mkk4a* and *mkk7* morphants (Fig. 3B). These data indicate that Mkk4b (exclusively) has a profound effect on CE, and that this effect is mediated through activation of the Jnk pathway. Thus, Mkk4b–Jnk signaling plays a critical role in proper CE movements during gastrulation.

To examine Mkk4b-Jnk signaling in zebrafish embryos, it was first necessary to identify zebrafish Jnk enzymes. To isolate zebrafish *jnk* genes, we used cDNA sequences for mammalian Jnks to perform BLAST searches of the zebrafish genomic database and identified four zebrafish *jnk* genes. A phylogenetic analysis based on the aa sequences of vertebrate Jnks revealed that the four zebrafish Jnk homologs closely resembled members of the three mammalian Jnk subfamilies, Jnk1, Jnk2, and Jnk3. We therefore designated the zebrafish proteins as Jnk1a-1, Jnk1a-2, Jnk2, and Jnk3 (Fig. S6). During gastrulation, mRNAs for Jnk1a-1, Jnk1a-2, and Jnk2 (but not Jnk3) were transcribed (data not shown).

To ascertain the functional importance of these zebrafish Jnk(s) for normal CE movements, we performed MO-mediated knockdown of the *jnk1a-1*, *jnk1a-2*, and *jnk2* genes and analyzed residual expression by RT-PCR. Co-injection of *jnk1a-1* MO and *jnk1a-2* MO efficiently prevented the correct splicing of *jnk1* pre-mRNAs during gastrulation (Fig. 3C). However, unlike the *Xenopus* Jnk1 morphant [Yamanaka et al., 2002], *jnk1a-1* and *jnk1a-2* morphants showed no gross morphological abnormalities (Fig. 3E, center), and the expression patterns of *hgg1*, *dlx3*, *ntl*, and *pax2.1* were completely normal (Fig. 3F, center). On the other hand, injection of *jnk2* MO not only prevented correct splicing of *jnk2* pre-mRNA (Fig. 3D) but also induced severe defects in anterior–posterior extension and mediolateral convergence, as assessed by analysis of morphology and molecular markers (Fig. 3E,F, right). These results indicate that Jnk2, but no form of Jnk1, is required for normal CE movements during zebrafish gastrulation.

TRANSCRIPTION OF ZEBRAFISH *WNT11* IS REPRESSED BY *MKK4B–JNK* SIGNALING

The molecular mechanism by which Jnk regulates CE movements is poorly understood. To identify relevant transcriptional targets downstream of the Mkk4b–Jnk signaling cascade associated with zebrafish CE, we used RT-PCR to survey mRNA levels of candidate genes in control and Mkk4b morphants at 75% epiboly (8 hpf). Because normal gastrulation requires modulation of cadherin-mediated cell–cell adhesion, we first investigated *e-cadherin* expression but found that its mRNA levels were unchanged in our morphants (Fig. 4A, row 1). Similarly, although *stat3* and *liv1* are reportedly essential for zebrafish gastrulation [Yamashita et al., 2004], the expression of these mRNAs was also normal in our *mkk* morphants (Fig. 4A, rows 2 and 3). We next screened components of the non-canonical Wnt pathway and found that, although *wnt5* expression was normal (Fig. 4A, row 4), *wnt11* expression was highly upregulated in Mkk4b-depleted embryos at 75% epiboly (8 hpf) (Fig. 4A, row 5), as well as at the 30% epiboly, shield, and tailbud stages (Fig. 4B, left). In contrast, upregulation of *wnt11* expression was not detected in Mkk4a- or Mkk7-depleted embryos (Fig. 4A). When we analyzed the expression of *wnt11* transcripts using quantitative real-time RT-PCR, we confirmed that levels

Fig. 2. Mkk4b–Jnk signaling is required for proper CE movements. A: Validation of *mkk4b* MO efficacy. The *mkk4b* MO targets the exon 6/intron 6 junction of *mkk4b* pre-mRNA as shown in the diagram (top). WT zebrafish embryos were injected with 0.8 pmol of *mkk4b* MO or control MO, and total RNA was extracted from the 30% epiboly to tailbud stages and subjected to RT-PCR analysis (bottom). Arrows in the diagram represent the primer pairs used for the RT-PCR analysis. The *mkk4b* MO efficiently prevents correct splicing of *mkk4b* pre-mRNA beginning at the shield stage (6 hpf), conceivably leading to a functional impairment of Mkk4b. B: Gross appearance of *mkk4b* MO-injected embryos. Images of a live control MO-injected embryo and live *mkk4b* morphants injected with the indicated doses of *mkk4b* MO were acquired at 11, 16, and 24 hpf (rows 1, 2, and 4, respectively). These embryos are viewed laterally, with anterior to the top. *Mkk4b* morphants exhibit a shortening of body length and brain degeneration in a MO dose-dependent manner. Row 3 shows that the notochord and somites are wider in the *mkk4b* morphant than in the control at 16 hpf (dorsal view). Scale bars = 200 μm (row 1); 200 μm (row 2); 50 μm (row 3); 500 μm (row 4). C: Quantification of anterior–posterior axis extension and mediolateral convergence at 16 hpf. Left panel shows the average angle between the anterior and posterior ends of embryos (n = 44, 36, 38) that were injected as indicated. Right panel shows the average mediolateral width of embryos (n = 44, 36, 38) that were injected as indicated. Data shown are the mean ± SEM. $^{*}P < 0.01$ versus control. D: Impaired CE in *mkk4b* morphants. Control MO-injected embryos and *mkk4b* morphants were analyzed by whole-mount in situ hybridization for the expression of tissue-specific genes at the tailbud stage (10 hpf). The position of the prechordal plate (*hgg1*) is more posterior and broader in *mkk4b* morphants compared to the control. Expression of *dlx3* (neuroectoderm) reveals a broader neural plate, and the notochord (*ntl*) is shorter and broader. The midbrain/hindbrain boundary (*pax2.1*) has expanded laterally. E: Normal rhombomeres in *mkk4b* morphants. WT embryos and *mkk4b* morphants had the same number and shape of rhombomeres (*krox20*) and somites (*myoD*) at the eight-somite stage (13 hpf), although the body axis was shorter and somites were wider in the *mkk4b* morphants. F: Expression of the dorsoventral patterning marker gene *gsc* is normal in *mkk4b* morphants. Control MO (0.8 pmol) or *mkk4b* MO (0.8 pmol) was injected into 1- to 4-cell embryos, which were analyzed by whole-mount in situ hybridization at the shield stage. Shown are animal pole views with dorsal to the right. For B and D–F, results shown are one experiment representative of at least three trials. G: Validation of *mkk7* MO efficacy as for A. Top: The *mkk7* MO targets the exon 9/intron 9 junction of *mkk7* pre-mRNA as shown in the diagram. Arrows represent primer pairs used in RT-PCR analysis. Bottom: The *mkk7* MO (0.8 pmol) causes a marked reduction in *mkk7* expression beginning at the shield stage (6 hpf). H: Gross appearance of *mkk7* MO-injected embryos. Images of a live untreated WT embryo and *mkk7* morphants injected with the indicated doses of *mkk7* MO were acquired at 24 hpf. All embryos are viewed laterally, with anterior to the top. *Mkk7* morphants exhibit weak, MO dose-dependent defects in the morphogenesis of the somites and a slightly shortened body length. I: Normal CE in *mkk7* morphants. WT embryos and *mkk7* morphants were analyzed for tissue-specific gene expression as for D. Even at a high dose of *mkk7* MO (1.5 pmol), the expression patterns of all tissue-specific genes examined were normal. J: Impaired somitogenesis in *mkk7* morphants. Top: The morphologies of rhombomeres (*krox20*) and somites (*myoD*) were examined at the eight-somite stage (13 hpf) in WT embryos and *mkk7* morphants. The body axis was shorter and the somites were wider in the latter (dorsal view). Bottom: Images of a live WT embryo (left) and live *mkk7* morphant (right) were acquired at 16 hpf (lateral view).

of *wnt11* mRNA were increased in *mkk4b* morphants (Fig. 4C). On the other hand, Mkk4b knockdown did not affect *wnt5* expression at any stage (Fig. 4B, right). These data indicate that Wnt11 itself is one of the molecular components downstream of the Jnk cascade in the non-canonical Wnt pathway associated with early embryogenesis.

We next examined whether activation of the Mkk4b–Jnk signaling pathway was sufficient to repress *wnt11* expression. Overexpression of a constitutively active form of Mkk4b (caMkk4b) markedly reduced the level of *wnt11* expression at 50% epiboly (Fig. 4D), reinforcing the notion that *wnt11* is a transcriptional target downstream of the Mkk4b–Jnk signaling cascade.

OVEREXPRESSION OF *WNT11* INDUCES ABNORMAL CE MOVEMENTS

To ascertain whether the increased *wnt11* expression in *mkk4b* morphants induced CE defects, we injected WT embryos with *wnt11* mRNA. Embryos overexpressing *wnt11* mRNA showed a shortening